Niedersachsen Ports

Niedersachsen Ports GmbH & Co. KG | Postfach 2044 | 26700 Emden

TU Delft / Faculty of CITG
Department of Geoscience & Engineering
Stevinweg 1
2628 CN Delft
P.O. Box 5048
2600 GA Delft

Aiko Hollander
Branch Manager

Niederlassung Emden
Friedrich-Naumann-Straße 7 – 9
26725 Emden

T +49 (0) 4921 897-100
F +49 (0) 4921 897-137
ahollander@nports.de

Emden, 18th December 2024

Clarification Statement regarding the bachelor's thesis "Seasonal Impact on Carbon Generation in Emden's Port – Examining Temperature-Driven Methane and Carbon Dioxide Formation in Fluid Mud"

Dear Sir/Madam,

We, as the operators of the Port of Emden, Niedersachsen Ports GmbH & Co. KG, would like to provide context regarding the scope and limitations of this bachelor's thesis, which represents an initial academic investigation into a complex operational environment.

This bachelor's thesis investigates gas production from fluid mud material through microbiological activity, based on laboratory experiments with subsequent extrapolation to the port environment. Gas production through microbial activity in fluid mud is a natural, continuous process independent of dredging activities, which are necessary to maintain water depth and port accessibility. However, it is important to recognize that dredging may alter the environmental conditions influencing these biochemical processes, something that was not addressed in the thesis. Therefore, the calculated emissions do not represent those directly caused by maintenance dredging, and the effects of dredging were not considered in this study. It is important to note that this study employed several simplifying assumptions necessary for an initial academic investigation. These simplifying assumptions include:

- A uniform fluid mud layer thickness across the inner harbour
- Laboratory conditions that may differ from actual field conditions
- Focus on a specific area of the port, excluding the outer harbour with its distinct environmental characteristics
- Production of methane as product of organic matter degradation, assuming a strict anaerobic fluid mud medium

These simplifying assumptions were necessary given the thesis's scope as a first independent research project. However, future quantitative assessments of greenhouse gas emissions would require case-specific analysis and validation of these assumptions.

We trust that these considerations will be taken into account when critically evaluating this work, particularly regarding its citation, reproduction of calculated values, and potential further analysis

Niedersachsen Ports

or use. We emphatically recommend consultation and exchange with Niedersachsen Ports to ensure the accuracy and practical relevance of any future research findings. Furthermore, any interpretations or potential applications should be rigorously cross-referenced with current operational practices and port management protocols to prevent misunderstandings or inappropriate extrapolations.

Kind regards,

i. V.
Aiko Hollander
Branch Management Emden

i. V.
Aike Wollersheim
Head of Technology / Railway Management Emden

Seasonal Impact on Carbon Generation in Emden's Port

Examining Temperature-Driven Methane and Carbon Dioxide Formation in Fluid Mud

Niek Appels

Delft University of Technology

TU Delft

Seasonal Impact on Carbon Generation in Emden's Port

Examining Temperature-Driven Methane and Carbon Dioxide Formation in Fluid Mud

by

Niek Appels (5403537)

In partial fulfilment of the requirements for the degree of

Bachelor of Science
in Civil Engineering

Supervisor 1:	Dr. habil. Julia Gebert
Supervisor 2:	Dr. Alex Kirichek
Project Duration:	April, 2024 - June, 2024
Faculty:	Civil Engineering and Geosciences, Delft
Date:	Monday 20th January, 2025

Cover Picture: Emden Dockyard. (2024, March 29). Bulk carrier SANDNES. https://www.emden-dockyard.com/bulk-carrier-sandnes/

TU Delft

Preface

Before you lies the Bachelor Thesis “Seasonal Impact on Carbon Generation in Emden’s Port: Examining Temperature-Driven Methane and Carbon Dioxide Formation in Fluid Mud”. This thesis was written to fulfill the graduation requirements for the Civil Engineering Bachelor of Science degree at TU Delft in Delft, the Netherlands. I worked on this thesis from April to June 2024.

Before starting this final project of my bachelor’s degree, I wasn’t entirely sure what topic I wanted to research. And although carbon production from sediment in a port might not immediately seem like a typical civil engineering subject, I was motivated by the opportunity to learn about a highly relevant, new topic. I am glad to have chosen this subject, as it has deepened my understanding and enthusiasm for sediment-related studies.

I owe deep gratitude to my supervisor, Dr. habil. Julia Gebert, whose guidance, support and feedback turned out to be crucial to the completion of this thesis. I also want to thank Dr. Alex Kirichek for agreeing to be my second supervisor and for taking the time to read and grade this thesis.

Finally I would like to thank you, my reader: I hope you enjoy this piece of work.

Niek Appels
Delft, January 2025

Abstract

In the Port of Emden, maintenance of the nautical depth is carried out by continuous re-circulation of sediment, creating a navigable fluid mud layer in the water and thereby facilitating safe navigation for ships. The sediment naturally contains organic matter, which to a certain extent is degradable by sediment microorganisms. Depending on the availability of oxygen, the degradation process generates carbon dioxide only (aerobic conditions) or methane and carbon dioxide (anaerobic conditions). This thesis aims to quantify the production of carbon dioxide and methane from fluid mud in the Port of Emden and analyze its seasonal variability to support carbon footprinting of sediment management activities.

In this thesis, an experiment was carried out to determine the carbon production of Emden samples at different temperatures. Results were used and, based on the fluid mud temperatures throughout the year, monthly carbon production was calculated. These values were adjusted for seasonal variations in organic matter availability and finally extrapolated to give the total monthly carbon production for the port. Using data from previous research, upper and lower bounds for this production were found.

The findings indicate that carbon production in the Port of Emden, due to micro-organisms in the fluid mud layer, varies significantly over the year. Specifically, the generated carbon was found to differ between 243 tons in February and 958 tons in August, with the upper bound being 7.2 times greater than these values and the lower bound 1.3 times smaller. From April until October, carbon generation was found to be considerably higher than from November until March, due to higher water temperatures and likely a greater availability of organic matter. Finally, the carbon production under aerobic conditions was found to be 2.7 to 2.8 times greater than under current conditions, with similar seasonal variability.

Limitations of this thesis include assumptions about uniform seasonal scaling of organic matter availability and incomplete data on fluid mud temperature variations across the year. Future research could address these limitations by gathering and incorporating more data on these parameters. Finally, future studies should focus on applying the findings of this thesis to explore strategies for reducing the carbon footprint of sediment management activities.

Contents

Preface i

Abstract ii

1 Introduction 1

2 Background 3
2.1 Fluid mud . . . 3
2.2 Decay of sedimentary organic matter . . . 4
2.2.1 Aerobic conditions . . . 4
2.2.2 Anaerobic conditions . . . 5

3 Study area 7
3.1 The Port of Emden . . . 7
3.2 Location of interest . . . 7
3.3 Boundary conditions . . . 8
3.3.1 The fluid mud layer . . . 8
3.3.2 Presence of oxygen . . . 9

4 Methodology 10
4.1 General approach . . . 10
4.2 Fluid mud temperature . . . 10
4.2.1 Surface water temperature . . . 11
4.2.2 Depth-correction . . . 11
4.3 Relation between temperature and carbon generation . . . 12
4.3.1 Experimental methods . . . 12
4.3.2 Data processing . . . 14
4.3.3 Data analysis . . . 15
4.3.4 Monthly carbon production . . . 15
4.3.5 Upper and lower bounds . . . 16
4.4 Conversion to port conditions . . . 16

5 Results 17
5.1 Fluid mud temperature . . . 17
5.1.1 Surface water temperature . . . 17
5.1.2 Relation between temperature at water surface and in fluid mud . . . 17
5.1.3 Goodness of fit . . . 18
5.1.4 Temperatures of the fluid mud layer . . . 18
5.2 Relation between temperature and carbon generation . . . 20
5.2.1 Results experiment . . . 20
5.2.2 Monthly carbon production . . . 22
5.2.3 Upper and lower bounds . . . 23
5.3 Conversion to port conditions . . . 24
5.3.1 Accounting for availability of organic material . . . 24
5.3.2 Extrapolation to the dimensions of the whole port . . . 25

6 Discussion 27
6.1 Relation between temperature and carbon generation . . . 27
6.2 Relation between available biomass and carbon generation . . . 27
6.3 Fluid mud temperature . . . 28
6.4 Limitations . . . 28

7 Conclusions and Recommendations **29**
7.1 Conclusions 29
7.2 Recommendations 30

References **31**

A Aerobic results **33**
A.1 Found carbon production 33
A.2 Upper and lower bounds 34
A.3 Conversion to port-conditions 35

B Python code **37**
B.1 Water temperatures 37
B.2 Monthly carbon production 38

C Raw data **42**

D Used results from previous research **45**

1

Introduction

In order to guarantee the accessibility of a port, a minimum navigable depth should be maintained. In the Port of Emden, this is achieved by a so-called re-circulation process in which the sediment is dredged with a trailing suction hopper dredger (TSHD) and then, in contrast to typical dredging operations, is not shipped away but is re-allocated to the water body at the same location. It is assumed that the contact with oxygen in the hold of the dredger and in the water phase supports a specialized microbial community whose production of extracellular polymeric substances (EPS) prevent the sediment from settling (Gebert et al., 2023). When compared to solid sediment, the process of re-circulation leads to lower yield stresses and densities, which ultimately allows for safe navigation and manoeuvring in the Port of Emden (Gebert et al., 2023).

As any dredging process, maintenance of the fluid mud layer contributes to the emission of greenhouse gases of the port (Niedersachsen Ports, n.d.). This is due to the emission from the fossil fuel consumption of the dredgers and other equipment that is used; however, the fluid mud layer itself also generates greenhouse gases, more specifically methane and carbon dioxide, through the natural biological breakdown of sediment organic matter (Li, 2019). Right now, these two gases are the top two contributors to climate change (NASA, 2023). This highlights the importance of knowing how much carbon dioxide and methane are produced. In this thesis, 'methane and carbon dioxide' is often shortened to simply 'carbon'. These two terms are used interchangeably and denote the same concept (carbon as contained in $\mathrm{CH_4}$ + $\mathrm{CO_2}$).

In previous research, the carbon generation for samples taken in Emden has been found (Gebert et al., 2023). This does however not give sufficient information to draw conclusions on the carbon production for the whole port and furthermore, results are only available for carbon production at 20 degrees. However, the temperature of the water and sediment in the port varies throughout the year, and the production of carbon dioxide and methane is known to be temperature-dependent. This makes an analysis of the seasonal variability of carbon generation in the port impossible.

The aim of this thesis is to quantify the production of carbon dioxide and methane from the biological breakdown of sediment organic matter for the whole Port of Emden and to analyse how this production varies over the year. The results of this research can be used as a basis for carbon footprinting of the sediment management activities in the Port of Emden.

The following research question is answered in this thesis: *What is the seasonal variability of methane and carbon dioxide generation from biodegradation of organic matter in the fluid mud in the Port of Emden?*

In order to answer this research question, a model was built that uses various sources of data retrieved by previous research. Also, an experiment was carried out, which provided data on the carbon production of Emden samples at different temperatures. The following sub-questions were used to come up with an answer to the main research question:

1. How does the fluid mud temperature vary throughout the year in the Port of Emden?
2. How do temperature variations influence methane and carbon dioxide generation in fluid mud in the Port of Emden?

3. How can the data on carbon generation per unit of dry weight be converted to a model for the whole port?

Before answering the sub-questions and research question, a hypothesis on the conclusions is given here.

First of all, it is expected that the fluid mud temperature in the summer and spring is significantly higher than in the winter and fall, due to the higher temperatures in those seasons. Furthermore, the expectation is that higher temperatures lead to a higher production of carbon dioxide and methane. This can for example be supported by the temperature coefficient (Q_{10}), a measure of temperature sensitivity of biochemical reactions. For most biological reactions, a temperature coefficient of around 2 or 3 has been found, which means that with every 10 °C increase in temperature, the reaction rate approximately doubles or triples (Reyes et al., 2008).

The hypothesis for the final sub-question, on the conversion of the data to the whole port, is that a factor should be applied that takes into account the availability of organic matter during the year, as the expectation is that there will be more organic matter available during the warmer months than in the colder months. Finally, the carbon production, found for a dry mass unit of fluid mud, can be multiplied by the dimensions of the fluid mud layer, to derive results for the whole port. By combining the hypotheses for the sub-questions, a hypothesis for the main research question can be formulated. Namely, the expectation is that a higher water temperature in the spring and summer will lead to higher carbon production in the port in those periods of the year and that therefore the carbon production in the winter and fall will be considerably lower.

In the next chapter of this thesis, first some background is provided on the specifics of fluid mud as well as the decomposition of organic matter. Then, in chapter 3, the area of interest for this research is defined followed by chapter 4, in which the methodology is lined out. In chapter 5, the results of the methods are shown followed by a discussion and conclusion.

2

Background

In this chapter, background is provided on some important definitions that are used in later chapters. First, the concept of fluid mud is explained and in the final two paragraphs, the decomposition of organic material is discussed.

2.1. Fluid mud

Fluid mud is a dense suspension of fine-grained sediments in water, where the close packing of sediment grains and flocks prevents them from settling easily. However, the potential for mobility is still present in fluid mud since the bonds are not strong enough to eliminate this (McAnally et al., 2007).

This mixture can form in rivers, lakes or estuaries where the amount of fine sediment entering the near-bed layer is greater than the dewatering rate of the high-density suspension (van Rijn, 2023). Fluid mud includes a wide range of sediment concentrations, typically from tens to hundreds of grams per liter, with bulk densities between 1080 and 1200 kg/m^3. The solid part primarily consists of clay- and silt-sized particles, typically defined as particles with a diameter of less than 62.5 μm (McAnally et al., 2007). The amount of water in fluid mud varies and therefore also the density varies, but is limited by the densities of water (lower limit) and solid sediment (upper limit). These limits also hold for the viscosity of fluid mud (McAnally et al., 2007).

In figure 2.1, a sample of fluid mud is shown (Gebert, n.d.). From the figure, it can be seen that this sample is fluid, but it does not seem as fluid as pure water. This illustrates the fact that the viscosity of fluid mud falls somewhere between that of water and solid sediment.

Figure 2.1: A fluid mud sample (Gebert, n.d.)

Moreover, fluid mud is a non-Newtonian fluid, in other words it does not follow Newton's law of viscosity, meaning the viscosity is dependent on the applied stress. More specifically, the rheological properties of fluid mud such as viscosity and yield stress are dependent on the stress history (van Rijn, 2023). This is the reason why constant re-circulation, as is done in the Port of Emden, leads to a lower viscosity and thus a better navigability of the fluid mud.

Finally, fluid mud consists partly of organic matter. The decomposition of this organic matter is the cause of carbon dioxide and methane generation. In the next sections, more background information on this organic decay is given.

2.2. Decay of sedimentary organic matter

Generally, organic decomposition is the disintegration of organic matter by a variety of microorganisms. This organic matter is most often plant-material that has undergone photosynthesis, thereby producing biopolymers and oxygen under the influence of sunlight and by capturing carbon dioxide (Bidlingmaier, 2016). The degradation of these polymers (such as lipids, proteins and carbohydrates) consists of multiple enzymatic reactions and, depending on the pathway, carbon dioxide and methane are produced (Arndt & LaRowe, 2017). It is important to note that organic material can be degraded with or without the presence of oxygen, which is called aerobic and anaerobic decay, respectively.

2.2.1. Aerobic conditions

Specifically, aerobic decay can be seen as the opposite to photosynthesis. After all, the biopolymers that are produced during photosynthesis are degraded during aerobic decomposition. Moreover, oxygen is consumed, carbon dioxide and water are produced and stored energy is released, which is opposite to what happens during photosynthesis (Bidlingmaier, 2016).

The chemical reaction that takes place differs depending on the organic matter that is degraded. But, in equation 2.1 the general scheme is shown (Bidlingmaier, 2016).

$$\textit{Organic matter} + \mathrm{O_2} \longrightarrow \mathrm{CO_2} + \mathrm{H_2O} + (\mathrm{N} + \mathrm{S} + \mathrm{P}) + \textit{energy} \tag{2.1}$$

As can be seen in equation 2.1, in addition to carbon dioxide and water, possible products of aerobic decomposition are nitrogen, sulfur and phosphorus. These elements can be part of the chemical reaction if the biopolymer that is decomposed contains one of such elements. For instance, if the organic matter contains a nitrogen element, ammonia ($\mathrm{NH_3}$) is produced (Bidlingmaier, 2016). However, since this thesis only focuses on the production of carbon dioxide and methane, these products will not be discussed further.

The process

Microorganisms play an important role in the aerobic decay of organic matter, more specifically biopolymers such as lipids, proteins and carbohydrates. These polymers are, however, often too large for microorganisms to be taken up. This is why the first step in aerobic digestion of biopolymers is the hydrolysis of ester bonds, glycoside bonds and peptide bonds (Polman et al., 2021). In biopolymers, component monomers are bonded via ester, glycoside, and peptide bonds, and therefore, after the hydrolysis of these bonds, the biopolymers are decomposed into monomers or smaller polymers.

Because of the size of the biopolymers, this first step needs to take place outside of the microorganism. In order to do this, microorganisms secrete extracellular enzymes that catalyze the mentioned hydrolysis (Polman et al., 2021). Once this first step has taken place, the smaller, soluble parts, are transported into the microorganism. Within the organism, the compounds are further digested by endoenzymes. Most microorganisms use multiple enzymes in order to fully decompose the substrate into carbon dioxide and water. All these enzymes are together called a system (Polman et al., 2021).

Up until now, the biotic parts of aerobic decay have been outlined, since all steps are related to living creatures in the form of microorganisms. However, abiotic processes also occur and break down the organic matter. Abiotic processes are not directly linked to the presence of oxygen and are therefore not necessarily relevant for aerobic decomposition only. However, in nature, anaerobic decay typi-

cally takes place in environments with limited sunlight penetration and under lower temperatures than aerobic decomposition, which is why they are discussed here.

Examples of abiotic processes are photodegradation and chemical hydrolysis under high temperatures or acidic/basic conditions (Polman et al., 2021). In photodegradation, organic matter is broken down by exposure to sunlight, especially UV radiation. Photons are absorbed by the polymers, which can cause polymer chains to cleave (Singh & Sharma, 2008). And under the presence of high temperatures or acidic/basic conditions, bonds are cleaved because the kinetic energy is increased (high temperatures) or because ions catalyze the hydrolysis reaction (acidic/basic conditions) (Singh & Sharma, 2008). However, since the fluid mud layer is located at a significant depth from the water surface in the Port of Emden, sunlight is unlikely to penetrate and high temperatures are unlikely to occur, making chemical hydrolysis under acidic/basic conditions the most relevant abiotic process in practice.

2.2.2. Anaerobic conditions

Under anaerobic conditions, so in the absence of oxygen, organic matter is degraded by micro-organisms and methane ($\mathrm{CH_4}$) and carbon dioxide ($\mathrm{CO_2}$) are produced. This process consists of four steps: hydrolysis, acidogenesis, acetogenesis and methanogenesis.

Hydrolysis

The first step in the anaerobic digestion of organic matter is hydrolysis. This step can be seen as a biological 'pretreatment' of the substrate in which polymeric substances such as lipids, proteins and carbohydrates are broken down into smaller monomers by reacting with a molecule of water (Menzel et al., 2020).

The process is similar to that for hydrolysis in aerobic digestion, as described in paragraph 2.2.1. Similarly, microorganisms secrete extracellular enzymes that catalyze the reaction outside of the cell. The conversion is catalysed by three different enzymes: esterases, glycosidases and peptidases that respectively catalyse the conversion of ester bonds, glycoside bonds and peptide ponds (Sikora et al., 2017). Just like for aerobic hydrolysis, monomers or smaller polymers are created. The bacteria that are involved in the anaerobic hydrolysis are most commonly *Firmicutes, Bacteoidetes* and *Gammaproteobacteria* (Sikora et al., 2017).

Acidogenesis

As mentioned in the previous subparagraph, hydrolysis produces monomers. More specifically, the products are soluble organic monomers of sugars and amino acids. During acidogenesis, these products are degraded by bacteria to produce alcohols, aldehydes and volatile fatty acids that contain six or fewer carbons in their structure (Sudoe, 2022). Finally, $\mathrm{H_2}$ and $\mathrm{CO_2}$ are produced along with ammonia gas ($\mathrm{NH_3}$) and acetate ($\mathrm{C_2H_3O_2^-}$) (Kamusoko et al., 2022).

Acidogenic bateria can be either facultative or strict anaerobes. Facultative anaerobes can produce ATP if oxygen is present, but are also capable of switching to fermentation in the absence of oxygen. Strict anaerobes, on the other hand, die if oxygen concentrations become too high (Prescott et al., 1996). Some species of bacteria for this step include *Lactobacillus, Escherichia* and *Staphylococcus* (Kamusoko et al., 2022).

Acetogenesis

Methane-producing bacteria cannot directly utilize the products of acidogenesis and therefore a third step is needed before methane can be produced (Kamusoko et al., 2022). In the third step, acetogenesis, the products of acidogenesis and the residuals of hydrolysis are further degraded and acetic acid, $\mathrm{CO_2}$ and $\mathrm{H_2}$ are produced (Giard, 2011).

Methanogenesis

In the final step of anaerobic decomposition, acetate or $\mathrm{H_2/CO_2}$ is transformed into methane and carbon dioxide by methanogens, specific microorganisms that can produce methane. There are multiple methanogens that degrade different substrates, typically three main groups can be identified:

1. Acetoclastic methanogens that use acetate and H_2 as substrate;
2. Hydrogenotrophic methanogens using H_2 and CO_2;
3. Mixed function methanogens that can use either acetate or H_2 and CO_2 (Giard, 2011)

It is estimated that 70% (v/v) of methane is produced from acetate, so by the acetoclastic methanogens.

The specific reactions that occur depend on the subtrates that are broken down by the methanogens. However, the final step of the methanogenesis is independent of the substrate. In this step, methyl-coenzyme M ($CH_3\text{-}S\text{-}CoM$) and coenzyme B react to produce heterodisulphide ($CoM-S-S\text{-}CoB$) and methane. This final step is shown in equation 2.2 (Sikora et al., 2017).

$$CH_3\text{-}S\text{-}CoM + CoB \longrightarrow CoM-S-S\text{-}CoB + CH_4 \tag{2.2}$$

The total process of anaerobic decay has been outlined in the previous subparagraphs and from this, it can be seen that polymeric substances such as lipids, proteins and carbohydrates go through four steps and are ultimately transformed into methane and carbon dioxide.

3

Study area

In this chapter, the area that this thesis focuses on is defined. First, a short description of the Port of Emden is given, followed by the specific locations within the port that are within question. Then, some boundary conditions that hold for these locations are outlined.

3.1. The Port of Emden

The Port of Emden is, as the name suggests, located in Emden, a city in *Ostfriesland* in the far north-west of Germany. The city of Emden is located at the mouth of the river Ems, where this river, that runs through the north-west part of Germany, flows into the North Sea (Encyclopaedia Britannica, 2011).

This makes the Port of Emden a sea port, and in fact it is the third largest North Sea port in Germany. In 2023, 5.6 million metric tons of cargo was handled in the Port of Emden, of which the largest share (2.3 million metric tons) consisted of vehicles. Building materials and forest products are two other important types of cargo for the port, with respectively 1.0 and 0.4 million metric tons in 2023. Recently, the Port of Emden has also started focusing on cargo related to renewable energy, especially the shipment of wind energy facilities and the supply of offshore wind farms. Connections by rail, road and the waterway networks of both the Netherlands and Germany allow for shipping of all these types of cargo to and from the port (Niedersachsen Ports, 2024).

3.2. Location of interest

The Port of Emden consists of two parts: the Outer Port that is exposed to the tides of the North Sea, and the tide-independent Inland Port. The border between these two areas is marked by two locks, with the *Große Seeschleuse* (Big Sealock) being the most notable one (Niedersachsen Ports, 2024). In this thesis, the monthly carbon production will be determined for the Inland Port, an aerial view of this part of the port is shown in figure 3.1.

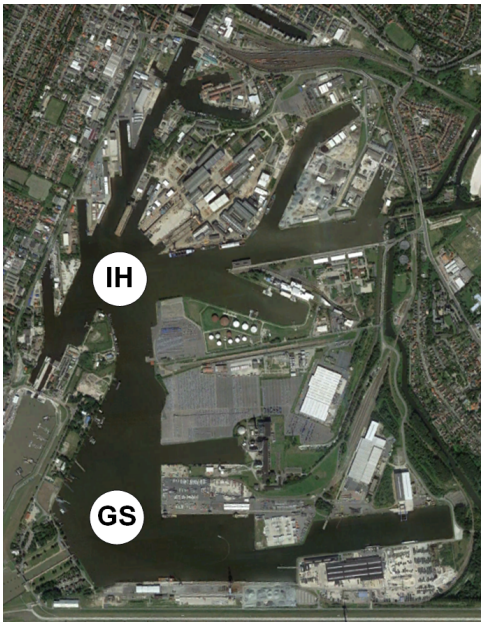

Figure 3.1: Aerial view of the Inland Port (GS = location Grosse Seeschleuse, IH = location Industriehafen) (Google Earth, 2019)

As can be seen in figure 3.1, the inner port is further subdivided into harbour basins, fairways, berthing areas and ship turning circles. The latter ones, *Grosse Seeschleuse*, located near the Big Sealock and *Industriehafen*, close to many warehouses, are focal points of dredging, as all ship traffic passes through them. These parts are indicated by GS and IH in figure 3.1, respectively.

3.3. Boundary conditions

For the area of the port as illustrated in figure 3.1, a couple of boundary conditions hold.

3.3.1. The fluid mud layer

First of all, the location and thickness of the fluid mud layer is an important factor. This is both known from previous research. In figure 3.2, the fluid mud layer is plotted. The upper line represents the lutocline, which is the interface between the water and fluid mud, and the lower line represents the fluid mud-bed interface, in other words the consolidated bottom of the port (Chamanmotlagh et al., 2024).

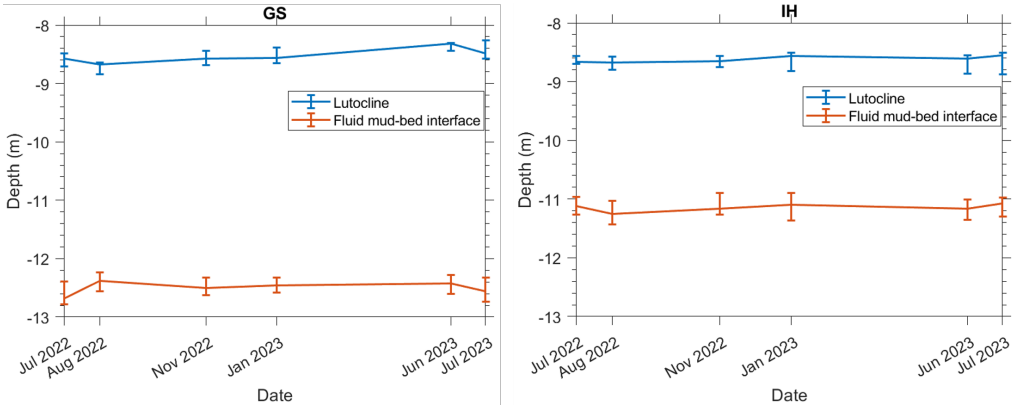

Figure 3.2: Location of the fluid mud layer (Chamanmotlagh et al., 2024)

On the y-axis of the plots in figure 3.2, the depth is shown in meters. So from these plots, the location and thickness of the fluid mud layer can be derived. By considering the two lines, it becomes clear that the fluid mud layer is located at a depth between ~8.5 m and ~12.5 m below the water surface for the *Große Seeschleuse* location and between ~8.5 m and ~11 m for the *Industriehafen*. By taking the difference in depth between the two lines in figure 3.2, it can be seen that the thickness of the fluid mud layer is around 4 m for the *Große Seeschleuse* location and around 2.5 m for the *Industriehafen*. From the figure, it can also be seen that depth and thickness of the fluid mud are very constant over time.

3.3.2. Presence of oxygen

As outlined in chapter 2, organic matter can be decomposed under aerobic or anaerobic circumstances, so either with or without the presence of oxygen. From previous research, the governing circumstances for the decomposition of organic matter can be derived.

In figure 3.3, the redox potential of the fluid mud at sites GS and IH is shown. Redox potential is a measure of the tendency of a chemical species to acquire or donate electrons, leading to reduction and oxidation, respectively. A negative redox potential indicates an environment where reduction reactions are favored and oxygen is absent or depleted. This typically signifies anaerobic conditions where alternative electron acceptors like nitrates, sulfates, or carbon dioxide are used by microorganisms. A positive redox potential, on the other hand, indicates an environment in which oxidation reactions are favored, meaning that oxygen is present (Mobilian & Craft, 2022).

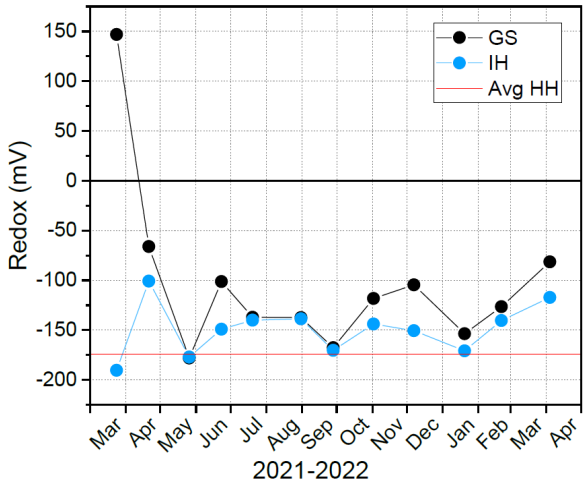

Figure 3.3: Redox potential of the fluid mud (Gebert et al., 2023)

From figure 3.3, it follows that the redox potential was negative for all samples apart from March 2021 at site GS (Gebert et al., 2023). This means that no oxygen was present in all but one sample. Therefore, anaerobic conditions hold for locations GS and IH, which is the area of interest.

Since the governing conditions in the Inland Port are anaerobic, this thesis will focus mostly on the generation of carbon under anaerobic conditions. The results have however also been derived for aerobic conditions, this is shown in appendix A.

4

Methodology

This chapter outlines the methods that were applied in order to answer the research question that was introduced in chapter 1: *What is the seasonal variability of methane and carbon dioxide generation from fluid mud in the Port of Emden?*

4.1. General approach

The general approach for finding an answer to the research question was to code an empirical model that calculates temperature-related carbon generation. For this, temperature functions were built that relate temperature to carbon generation per unit of dry weight of the sediment. The temperatures of the fluid mud over the year were found, which were put into the model to find the carbon generation per month. Finally, results were extrapolated to the whole port. In the following paragraphs, this methodology is outlined in more detail, first this is done for the fluid mud temperatures.

4.2. Fluid mud temperature

First, it should be known how the temperature of the fluid mud varies throughout the year. As was shown in chapter 3, the fluid mud layer lies between 8.5 m and 12.5 m below the water surface in the Port of Emden. Data on the water temperature at these depths is available, but only for six months. Therefore, based on this data only, no conclusions could be drawn for the remaining months. Instead, a different approach was chosen. Since data on the water temperature at the surface was available for the whole year, these results were analyzed first. Then, these results were corrected for the depth at which the fluid mud layer is located.

In this paragraph, some information on the availability of different datasets is given. First of all for the water temperature at the surface, but also in 4.2.2 for the availability of data on the water temperature over the depth of the port. Table 4.1 shows the availability of the different datasets. Columns ‘2022’ and ‘2023’ indicate the availability of data on the water surface for the months of those respective years and finally, ‘UPS’ is on the availability of temperature data over the water depth. In table 4.1, an ‘x’ indicates that a specific dataset was available. In the following sub paragraphs, the availability of the data is explained in more detail, among other aspects.

Table 4.1: Available datasets (x indicates availability)

	2022	2023	USP
Jan	x	x	
Feb	x	x	
Mar	x	x	
Apr	x	x	x
May	x	x	
Jun	x	x	
Jul	x	x	x
Aug	x	x	x
Sep	x	x	
Oct	x	x	x
Nov	x[1]		x
Dec	x[1]		x

4.2.1. Surface water temperature

Following this outlined approach, first the water temperature at the surface had to be known. The water temperature data at the surface level in the port of Emden was provided for 2022 and 2023. In both of these years, the temperature was measured monthly. In 2022, the temperature was measured at 24 different locations and in 2023 at 10 locations. The availability is shown in table 4.1.

In order to obtain a reliable value for the water temperature per month, the average of all locations was taken for both years. Then, for each month, the average of the temperatures for the two years was taken.

However, this procedure could not be applied in all cases, since the months during which measurements were carried out were not entirely the same for both datasets. This is because the dataset from 2023 contains measurements from November 2022 until October 2023, but the set on 2022 contains measurements from January until December of that year. Hence, there is no data from November and December 2023 and there are two datasets that give measurements for November and December 2022.

This means that, for November and December, data is available for one year (2022) but can be found in both datasets. While both datasets provide slightly different averages, the 2022 dataset offers measurements from more locations compared to the 2023 dataset (24 locations versus 10). Furthermore, these 10 locations are also included in the 2023 dataset. As a result, data from the 2022 dataset was used for November and December 2022.

4.2.2. Depth-correction

The water temperatures at the surface level could not be directly applied to the model, since the water temperatures at the depths of the fluid mud layer likely differ. Therefore, a correction was applied, but first the presence and size of this correction had to be determined.

In order to find this possible correction, the relationship between the water temperature at the surface and the temperature at the location of the fluid mud was examined. To find this relation, a total number of 192 datasets with measurements in the Port of Emden was used. These datasets contain measurements of the water temperature at different locations and at different water depths that were gathered by a USP.

Each dataset contains data on a specific month, the available months are: April, July, August, October, November and December. For clarity, available data is shown in table 4.1. The depth at which the temperature was measured varied between 2 m and 12.5 m below the surface and between 118 and 2718 measurements were carried out per database.

[1] Two datasets are available, with slightly different data.

In order to identify a possible relation between the water depth and water temperature in the Port of Emden, a scatter plot was created that relates the water temperature at depth -10 m (the average of the fluid mud layer depth) to the water temperature at -2 m. For this, the available measurements closest to 2 m and 10 m were taken from all databases.

For the relation, it was assumed that the water temperature at -2 m is equal to the water temperature at the surface. After all, the measurements were taken relatively close to the surface and by making this assumption, it is possible to correct the measured temperatures at the surface for the depth of the fluid mud layer. Furthermore, the temperature at depth -10 m was assumed to be representative for the whole fluid mud layer, since this is approximately the middle of the layer that is located between 8.5 m and 12.5 m below the water surface, as discussed in chapter 3.

Based on the measurements in the before mentioned scatter plot, a trend line could be fitted to the data. This trend line relates the temperature at depth -10 m to the temperature at -2 m. The validity of the fitted trend line was checked by Pearson's correlation coefficient, for this a level of significance of 0.1% was applied.

After checking the validity of the fitted trend line, the found temperatures at the water surface could be corrected for the depth.

4.3. Relation between temperature and carbon generation

After the temperatures in the fluid mud layer were determined per month, the amount of methane and carbon dioxide that is generated at these temperatures had to be determined. For this, a temperature function was created that relates the temperature to gas generation. By carrying out a series of experiments, such a temperature function was created.

4.3.1. Experimental methods

For the experiment, fluid mud that had been sampled from the location IH within Port of Emden by researchers from the project CIRCLEMUD (https://www.tudelft.nl/mudnet/projects/circlemud) was incubated at different temperatures, both under aerobic and anaerobic circumstances. A total of five different temperatures were examined and for each temperature, two aerobic and two anaerobic samples were used, leading to a total of twenty samples. The samples were kept at different temperatures and the gas composition was analyzed weekly. Below, various parts of the experiment are explained in more detail.

Sampling

Before the experiment could start, a mixed sample had to be prepared. Sampling at location had already been carried out, and sediment samples from different locations in the Port of Emden were available. All samples were taken in the *Industriehafen*, specifically from locations IHX62 and IHX43. At each of these two points, three samples covering the total thickness of the fluid mud layer were taken. All six samples were mixed to produce a mixed sample. The exact locations of sampling are indicated in figure 4.1.

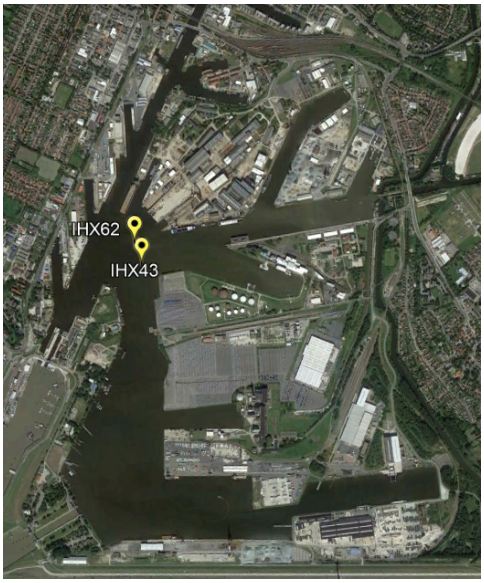

Figure 4.1: Locations IHX62 and IHX43 within the port (Google Earth, 2019)

Approximately 300 grams of sediment for every depth, for both locations, was taken and put together. After thorough mixing, the new sediment was put into the sampling bottles. For the aerobic samples, bottles of size 250 mL were used with approximately 15 grams of sediment in it and for the anaerobic samples the bottles had size 500 mL and 100 grams of sediment was used. The exact masses used for the sediment samples are shown in appendix C.

In order to ensure anaerobic circumstances, the 500 mL bottles were flushed with pure nitrogen during a duration of approximately 3 minutes. Furthermore, 30 mL of air was injected into the 250 mL samples to make sure no underpressure would occur for the aerobic samples. In figure 4.2, the flushing of the anaerobic samples (left) and pressurising of the aerobic samples (right) is shown.

Figure 4.2: Flushing the anaerobic samples and pressurising the aerobic samples [Author's photos]

The temperatures

A total of five different temperatures were used for the experiment, namely: 4, 8, 13, 20 and 25 °C. The exact temperatures were recorded during the experiment and are reported in the results.

Determining the gas composition

The gas composition and pressure were determined and recorded on a weekly basis using a gas chromatograph (GC-TCD, Da Vinci Laboratory Solutions) and pressure gauge (LEX1, Keller). The GC gave the volumetric percentage of $\mathrm{CO_2}$ and $\mathrm{CH_4}$ and the pressure was measured every time for each sample, both before and after sampling, by piercing a needle through the stopper. In appendix C the recorded compositions and pressures are shown.

4.3.2. Data processing

Data processing

After conclusion of the experiment, the gas composition results were converted into carbon release in absolute terms (g C/kg DW). First, the ideal gas law was used to determine the total carbon present in the headspace of the bottle.

The ideal gas law reads as follows:

$$n = \frac{P \cdot V}{R \cdot T} \tag{4.1}$$

With n the molaric amount of gas present, P the pressure [kPa], V the volume [mL], T the temperature in Kelvin and finally, R is the ideal gas constant (8.3144 $\mathrm{J \cdot mol^{-1} K^{-1}}$).

Equation 4.1 was filled in for all measurements, to determine the number of moles of both carbon dioxide and methane. Here, the pressures before sampling were used.

The volume of the generated carbon dioxide and methane had to be determined for all samples. For this, first the volume of the used bottles was determined, as well as the mass of sediment that was used for all samples. Some of the remaining sediment was then sampled and weighted, and afterwards was put into an oven for a day. By this, the dry weight and thus the water content of the sediment was calculated. With this, the volume of the water for each sample could be determined, as well as the volume of the total sample. By subtracting this from the measured volume of the bottle, the volume of the headspace was determined for all samples. This volume was multiplied by the percentage of $\mathrm{CO_2}$ and $\mathrm{CH_4}$ in the sample, as found by the GC, and filled into equation 4.1.

The temperature differed per sample but was recorded and afterwards converted into Kelvin. This was then filled into equation 4.1 as well. By this, the number of moles for both carbon dioxide and methane in the gaseous phase was known for all samples. These two values were added and, by using the molar mass of carbon and the amount of dry mass for all samples, this was converted into total grams of carbon per gram of dry weight.

This however still only gives information on the gaseous phase of the samples, but gases also have the ability to dissolve in water. For this, Henry's law was used:

$$S = K'_H \cdot P \tag{4.2}$$

With S the solubility in mol/m^3, K'_H Henry's constant (corrected for pH) and P the partial pressure for the gas in question. Henry's law was only filled in for $\mathrm{CO_2}$ and not for $\mathrm{CH_4}$. After all, the solubility for methane is only around 0.0227 g/kg, whereas the solubility of carbon dioxide is significantly higher at 1.50 g/kg (Haynes et al., 2014). Therefore, equation 4.2 was only filled in for carbon dioxide and thus the solubility of methane was ignored.

For all samples, the partial pressure of $\mathrm{CO_2}$ was determined by multiplying the percentage of $\mathrm{CO_2}$ as found by the GC, by the pressure of the sample that was determined before sampling. Then, the pH value of the samples was found, which was used to correct Henry's constant. More specifically, Henry's constant was corrected as follows:

$$K'_H = 1.82533 \times 10^{-10} \cdot e^{-x/-0.43293} + 3.94288 \times 10^{-4} \tag{4.3}$$

With x the pH as measured.

With this, equation 4.2 could be filled in for all samples, which resulted in the number of moles of dissolved CO_2 per cubic meter of water. By again using the molar mass of carbon and the volume of the water in all samples, this was converted into total grams of dissolved carbon per gram of dry weight.

Finally, the two results (carbon in gaseous phase and dissolved carbon) were summed and with this, the total generated carbon per gram of dry weight was known for all samples.

4.3.3. Data analysis

After processing of the raw data, plots were created that show the carbon release over time for different temperatures. For the Port of Hamburg, these plots are available from previous research.

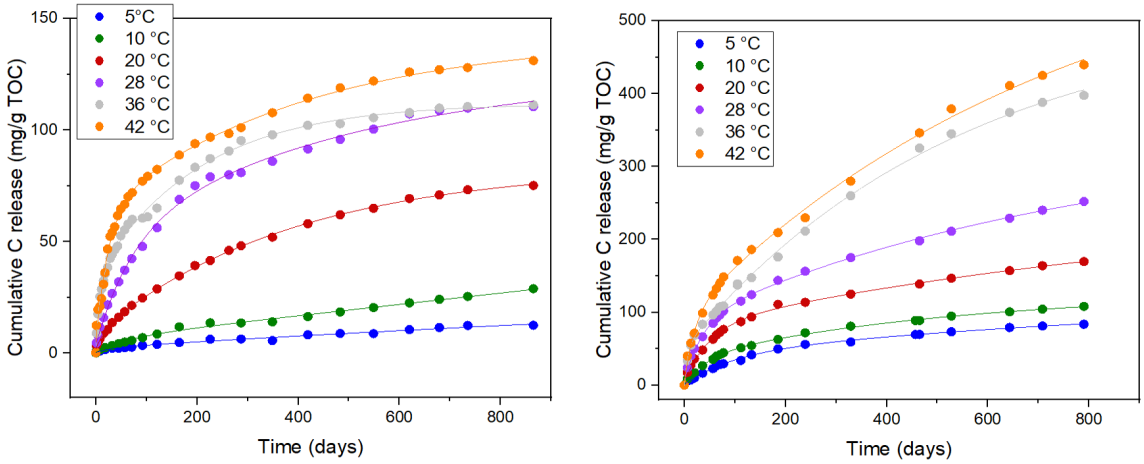

Figure 4.3: Plots showing the carbon release over time for different temperatures for the Port of Hamburg (Zander, 2022)

In figure 4.3, anaerobic conditions on the left and aerobic conditions on the right. As can be seen in the figure, the carbon release increases with an increasing temperature and is higher for aerobic conditions than for anaerobic conditions.

The data shown in figure 4.3 could not be directly applied to the Port of Emden, since the activity of the sediment is most likely different for this port. The functions can however be used to compare and verify the results that were derived in the experiment. For this, the generated carbon after 20 days was obtained from data gathered in the experiment, for different temperatures, and plotted against the temperature at which that specific sample was kept. This was also done for data that was gathered by Zander et al., 2022 on the Port of Hamburg. However, this study found carbon production after 21 days which is why these values were scaled to reflect the production after 20 days.

4.3.4. Monthly carbon production

After conclusion of the experiment, the cumulative produced carbon per gram of dry weight was known for the different temperatures over time. This information was used to determine the carbon production per month. The data could not be applied directly, since the in-situ conditions differ from the experimental conditions. After all, in a port, there is an influx of new organic material, which does not happen in the samples of the experiment. To reflect this reality, the cumulative carbon production after 5 days was used and multiplied to represent the total number of days in each month. This number of days was chosen, since the first days of the experiment often yield troubled data due to preparing and mixing of the sampling.

The real temperatures in the port of course differ from the temperatures that were researched in the experiment. Therefore, the real temperatures, as determined by the method that was outlined in paragraph 4.2, were compared to the nearest two available results. The weighted average was then taken, from which the carbon production after 5 days and finally the monthly production was determined for all ‘real temperatures’.

4.3.5. Upper and lower bounds

As mentioned before, previous research on the Port of Emden has resulted in data on the carbon production after 21 days at 20 °C (Gebert et al., 2023). This variable was measured for a total of thirty samples throughout the port, under both aerobic and anaerobic conditions.

This data allows for determining upper and lower bounds to the carbon production in the Port of Emden. For this, the amount of carbon produced after 21 days at 20 °C, as found in the experiment, was used. This value was then compared to the available data from the previous report, more specifically the minimum and maximum produced carbon after 21 days at 20 °C. A graph that displays the used data is shown in appendix D. This resulted in two scaling factors, based on the minimum and maximum produced carbon, as found by previous research. These same scaling factors were applied to the carbon production after 5 days, as found in the experiment. Then, the same procedure as described in paragraph 4.3.4 was applied to obtain minimum and maximum plausible values for the monthly carbon production.

4.4. Conversion to port conditions

Before extrapolating the carbon generation to the whole port, the results from the experiment were scaled to take into account the variability of the available biomass over the year. After all, in the warmer months, there is most likely more biomass available in the port, leading to more carbon production, than in the colder months. Since the samples used in the experiment were all sampled in April, this effect was not properly taken into account.

To determine the presence and magnitude of the scaling factor, the results as found by Gebert in 2023 were used. The exact results as found by Gebert are shown in appendix D. Specifically, the carbon production under aerobic circumstances during the warmest months was compared to the production during the coldest months of the year. Since those samples were all kept at 20 °C, any variance in the values was caused by a varying amount of organic matter. For determining the ‘warmest’ and ‘coldest’ months, the water temperatures as determined before were taken into account.

After this scaling factor was applied, it was known how much carbon is generated per gram of dry weight of sediment per month. This does however not give any information on the carbon dioxide and methane that is produced in the Port of Emden. Therefore, the results were extrapolated to the whole port.

In order to extrapolate the found values, the total dry weight of the fluid mud layer had to be determined. For this, the density of the fluid mud, as well as the area of the location of interest had to be found. The density of the fluid mud was measured by Gebert in 2023, for a total of 25 samples from both the *Industriehafen* and *Große Seeschleuse*. The average was taken to find a representative density for the whole area of interest, as defined in paragraph 3.2, the used value was 1.1 ton/m^3. For the same 25 samples, the dry mass content was measured as well (Gebert et al., 2023). To derive a representative value for the dry mass content, the average of all measurements was taken again.

From figure 3.2, it follows that the fluid mud layer has a thickness of approximately 4 meters in the ‘GS’ part of the port and 2.5 m in the ‘IH’ part. In this step, the average of these two values was taken to represent the thickness of the fluid mud layer over the whole port. Next, by using satellite images and area measurement software, the area of the location of interest was determined, which then allowed for the calculation of the volume of the fluid mud layer. The found volume was 5,590,000 m^3.

This found volume was multiplied by the determined density of the fluid mud to obtain the total mass of fluid mud in the port. This value was then multiplied by the average dry mass content, which resulted in the total mass of dry matter, in other words the total tons of dry weight of the fluid mud layer.

The final step in determining the carbon production of the fluid mud layer was to multiply the found values for carbon production per gram of dry weight by the now known total dry weight of the layer. The values in the table were determined in mg C/g DW, which after division by 1000, corresponds to ton C/ ton DW. Therefore, the recorded values were divided by 1000 and then multiplied by the dry weight of the fluid mud layer (in tons) to obtain the carbon production in tons.

5 Results

In this chapter, the results are presented and discussed. The results for each sub-question are presented, and then final results are shown.

5.1. Fluid mud temperature

5.1.1. Surface water temperature

As discussed in chapter 4, data on the water temperature at the water surface is available. The average for all available locations per month was taken, which gave the following temperatures:

Table 5.1: Water temperature (°C) at surface per month

	2022	**2023**	**Mean**
Jan	4.82	4.35	4.58
Feb	5.74	5.79	5.76
Mar	9.00	8.33	8.66
Apr	11.93	10.77	11.35
May	15.45	16.27	15.86
Jun	19.65	22.81	21.23
Jul	21.03	19.59	20.31
Aug	22.54	21.54	22.04
Sep	16.06	17.88	16.97
Oct	13.03	10.92	11.98
Nov	6.94		6.94
Dec	2.24		2.24

The final column in table 5.1 represents the average of the recorded surface temperatures in 2022 and 2023. For November and December, this average is equal to the measured value in 2022, as this is the only data available.

However, the sediment in question is of course not located at the water surface. In fact, as was shown in chapter 3, the fluid mud layer lies between 8.5 m and 12.5 m below the water surface. Since the fluid mud layer is located at a significant depth below the water surface, the temperatures from table 5.1 needed to be corrected for depth. First, the relation between the water temperature at the surface and the temperature of the fluid mud was found.

5.1.2. Relation between temperature at water surface and in fluid mud

In order to identify a possible relation between the water temperatures at the depth of the fluid mud layer and at the surface, a scatter plot was created, containing different measurements at depths 10 m and 2 m, as explained in chapter 4. The result is shown in figure 5.1. Here, the water temperature at -2 m was assumed to be equal to the temperature at the surface. In chapter 4, this is explained and supported in more detail.

In figure 5.1, the linear trend line that best fits the data is shown by the coloured line. The python code that was used to obtain the figure is shown in appendix B. In figure 5.1, the different coloured dots indicate during which season the measurement was taken, but this was not used in the methodology.

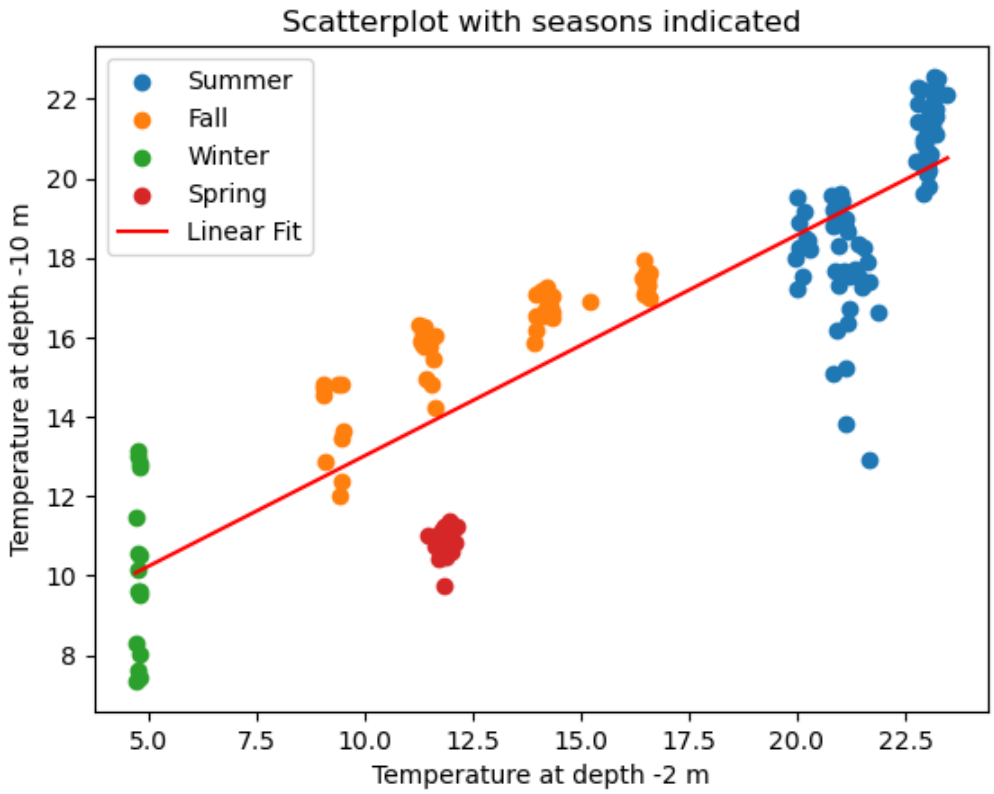

Figure 5.1: Scatter plot of temperature at fluid mud / at surface

5.1.3. Goodness of fit

Based on the scatter plot and trend line that were created, the temperatures at the water surface could be adjusted for the depth of the fluid mud layer. However, first the validity of the fit had to be checked. This was done by using the so-called R-squared value.

This R-squared is a measure to determine the goodness-of-fit for models. It represents the proportion of the variation in the dependent variable (temperature at depth -2 m) that is predictable from the independent variable (temperature at depth - 10 m).

The R-squared belonging to the linear fit was determined. In figure 5.1, this value is shown in the legend. As can be seen in figure 5.1, the value for R-squared is equal to 0.749, by taking the square root it follows that R is equal to 0.865. Pearson's Correlation table provides guidance on interpreting correlation strength. The fit in figure 5.1 is based on 177 measurements, which corresponds to 175 degrees of freedom. For this number of degrees of freedom and a level of significance of 0.001, the critical value from Pearson's Correlation table for R is 0.245, which is lower than the found value for R (0.865) (Zaiontz, n.d.). Therefore, the probability for this correlation to have occurred by chance is lower than 0.1%, indicating a strong relationship. Thus, the fits relating the temperature at depth -10 m to the temperature at depth -2 m could be accepted.

5.1.4. Temperatures of the fluid mud layer

The linear fit, as shown by the red line in figure 5.1, was found using the code shown in appendix B. The following function was found:

$$T_{-10}(T_{surf}) = 0.5566 \cdot T_{surf} + 7.4447 \tag{5.1}$$

With T_{surf} the water temperature at the surface, as mentioned before this temperature was assumed to be equal to the temperature at depth -2 m. Furthermore, T_{-10} is the water temperature at depth -10 m. Based on the found functions, the water temperatures at the surface as shown in table 5.1 could be corrected for the depth at which the fluid mud is located. This adjustment assumes that the temperature of the fluid mud is represented by the temperature at -10 meters, as explained in chapter 4.

Now, equation 5.1 could be filled in for the temperatures at the water surface that were found in table 5.1. This was done for all months, and in table 5.2, the resulting corrected temperatures are shown.

Table 5.2: Temperatures of the fluid mud layer

	Temperature (°C)
Jan	9.99
Feb	10.65
Mar	12.27
Apr	13.76
May	16.27
Jun	19.26
Jul	18.75
Aug	19.71
Sep	16.89
Oct	14.11
Nov	11.31
Dec	8.69

As can be seen by comparing tables 5.1 and 5.2, the applied correction varies per month. For January until May and October until December, the temperature of the fluid mud layer was found to be higher than the water temperature at the surface. These corrections vary between and 0.41 °C for May and 6.45 °C for December. For June until September, however, the temperature of the fluid mud layer was found to be lower than the temperature of the surface water. These corrections vary between 0.08 °C for September and 2.33 °C for August.

In figure 5.2, the results from table 5.1 and 5.2 are represented in a bar graph. This graph shows the average temperatures per month for both the surface water and the fluid mud layer.

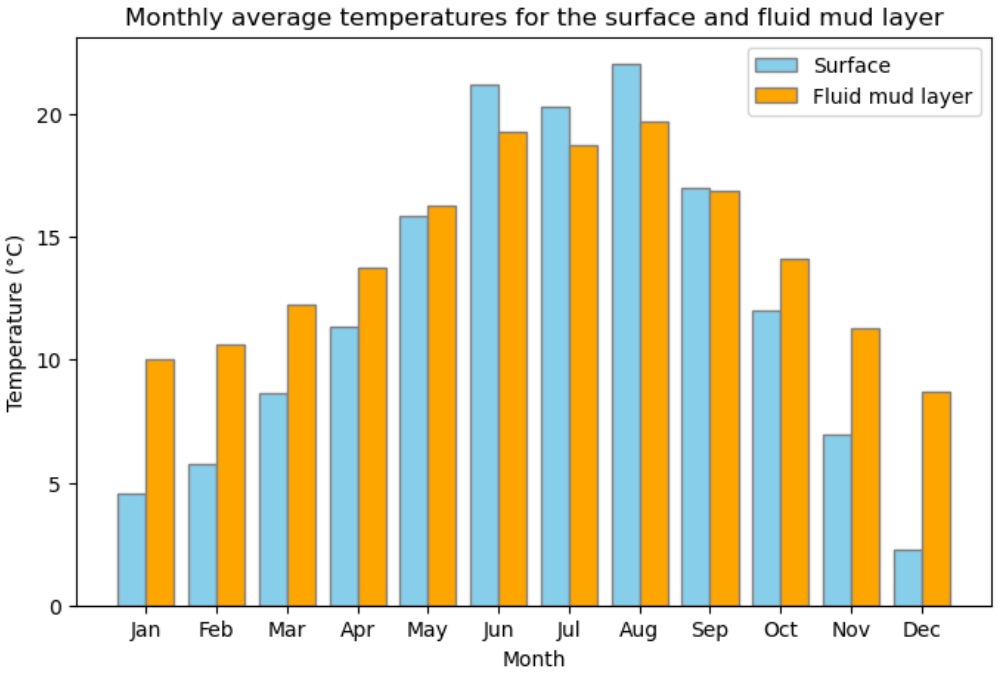

Figure 5.2: Surface water and fluid mud temperatures per month

5.2. Relation between temperature and carbon generation

In this chapter, unless specified otherwise, only the results for carbon generation under anaerobic circumstances are given, since these are the governing circumstances, as outlined in chapter 3. Aerobic conditions should however not be overlooked, since aerobic conditions could be relevant in the future. Therefore, the procedure that is outlined in paragraph 4.3 was applied for aerobic circumstances as well. The results are shown in in appendix A.

5.2.1. Results experiment

First, the found sample properties are shown in table 5.3. The acidity, gravimetric water content and redox potential were measured for the created samples in the experiment. The other properties were found by taking the average value for IH as found by Gebert et al., 2023.

Table 5.3: Found sample properties

Property	Found value	
Acidity	7.00	pH
Gravimetric water content	440.14	%
Redox potential	-115	mV
TOC	3.65	%
Density	1.11	ton/m^3
Clay content	6.21	vol.%
Silt content	84.02	vol.%
Sand content	9.77	vol.%

The raw data that was gathered in the experiment is displayed in appendix C, here the processed results are shown. The pH of the samples was found to be equal to 7.00, as was shown in table 5.3.

In figure 5.3, the resulting values for the generated carbon, as determined by the method described in chapter 4, are shown for both anaerobic and aerobic conditions. With this, plots such as the ones that are shown in figure 4.3, were retrieved, but now specifically for the Port of Emden.

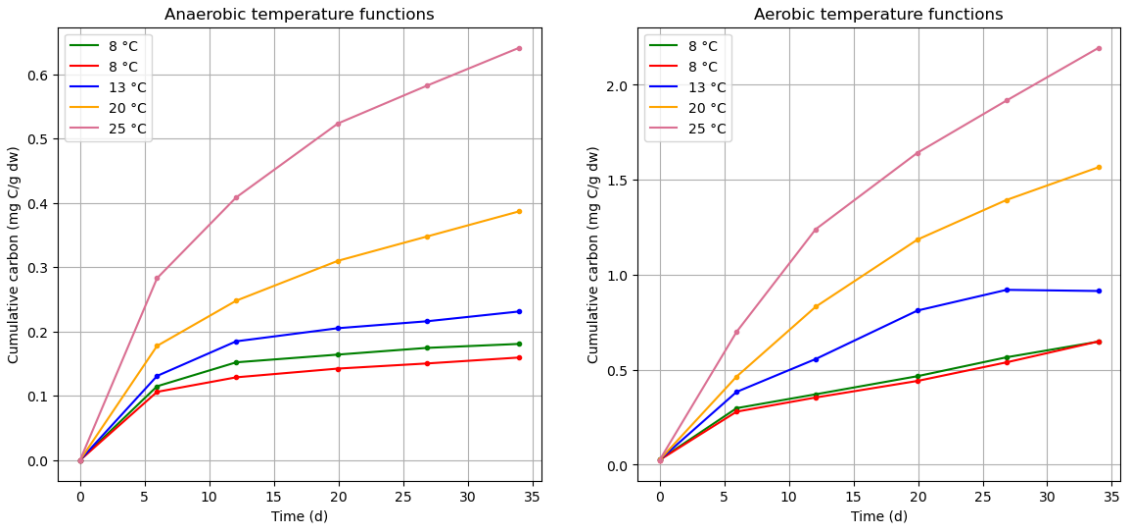

Figure 5.3: Plots showing the carbon release over time for different temperatures for the Port of Hamburg

As can be seen in figure 5.3, data was retrieved for 8 °C and there is no result for 4 °C, whereas this temperature is mentioned in chapter 4. This the result of an error in conducting the experiment. The samples that were supposed to be kept at 4 °C, were in fact kept at 8 °C, since the fridge in which the samples were kept turned out to be warmer than expected. This is why two results for 8 °C are available, but for further calculations, the average of the two results was taken.

Moreover, one of the parallel samples that was kept at 13 °C under aerobic conditions showed a declining carbon content after 20 days. Since this is impossible due to the air-tight cap on all samples, this was likely the result of human failure while conducting the experiment, which is why this parallel result was not taken into account. The other results in figure 5.3 are all based on two parallel samples. However, on general, by comparing the results from the two parallels for each temperature, it was found that the cumulative carbon generation calculated for the two parallels differed by less than 8% on average, with similar trends for each parallel.

The outcomes can be compared to the results that were obtained by Zander in 2022, for the Port of Hamburg. For this, the generated carbon after 20 days was compared for the different temperatures, both for the findings from Zander (21-day values, scaled) and from the experiment conducted in this thesis. The result is shown in figure 5.4. On the right-hand side of figure 5.4, the same analysis is shown, but here all values are scaled to the found carbon production after 20 days at 20 °C for the specific samples. This helps to see how the carbon production decreases, with a decreasing temperature.

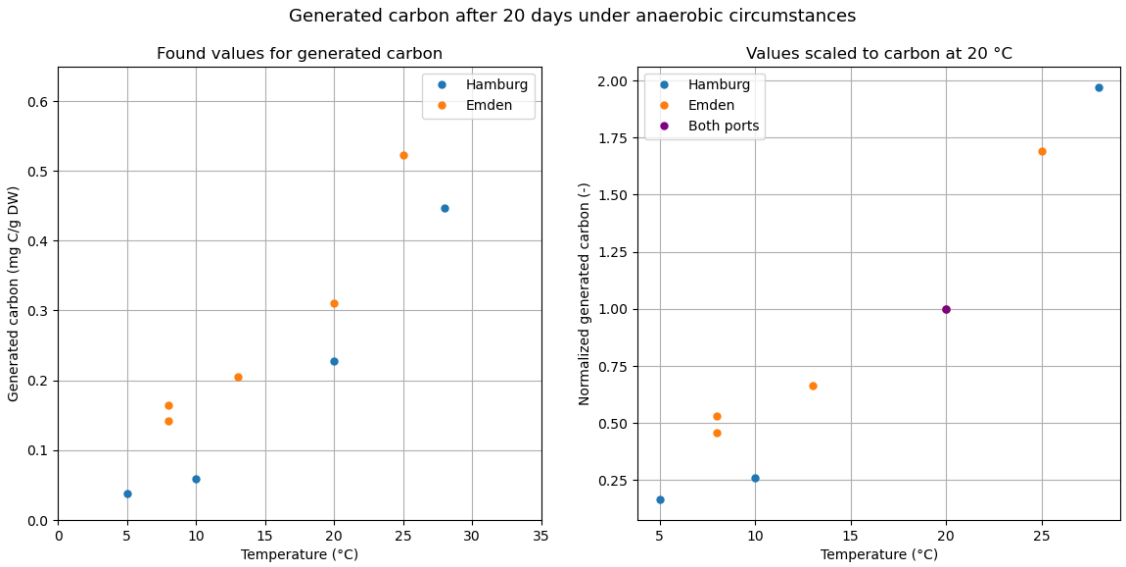

Figure 5.4: Comparison of Hamburg and Emden temperature functions for anaerobic circumstances

From figure 5.4, it follows that the samples from the Port of Emden were found to produce slightly more carbon for the same temperature than the samples from the Port of Hamburg, under anaerobic circumstances. However, the found amounts of carbon, if subjected to the same temperature, were similar. From the right graph, it can be seen that the samples react similarly to a change in temperature as well, since the slopes for both ports are similar. Furthermore, the right graph also shows that a temperature decrease of around 10 °C resulted in approximately half the carbon production, for the Emden samples. This corresponds to a Q_{10} of around 2.

5.2.2. Monthly carbon production

As explained in paragraph 4.3.4, the monthly production of carbon in the Port of Emden was determined by using the results from the experiment. For this, the cumulative carbon production after 5 days was used. In the experiment, measurements were carried out after 5.96 days. This data was used and scaled to reflect the total amount of carbon after exactly 5 days. By this, the following results for the carbon generation after 5 days were found, for the Port of Emden.

Table 5.4: Carbon production after 5 days under anaerobic circumstances

Temperature (°C)	Generated carbon (mg C/g DW)
8	0.0926
13	0.1098
20	0.1490
25	0.2373

In order to be able to find the carbon generation in the Port of Emden, the monthly fluid mud temperatures as found in table 5.2 were taken and compared to the nearest two available results in table 5.4. The weighted average was then taken, from which the carbon production after 5 days for all temperatures was determined. The result is shown in table 5.5. Then, these values were multiplied by a factor of 5.6, 6 or 6.2, depending on the total number of days in each month, to obtain the carbon production for that month. This is shown in the final column of table 5.5.

Table 5.5: Monthly carbon production under anaerobic circumstances

	Temperature (°C)	5-day generation (mg C/g DW)	Monthly generation (mg C/g DW)
Jan	9.990	0.100	0.617
Feb	10.650	0.102	0.570
Mar	12.270	0.107	0.665
Apr	13.760	0.114	0.684
May	16.270	0.128	0.794
Jun	19.260	0.145	0.869
Jul	18.750	0.142	0.880
Aug	19.710	0.147	0.914
Sep	16.890	0.132	0.789
Oct	14.110	0.116	0.719
Nov	11.310	0.104	0.624
Dec	8.690	0.095	0.589

5.2.3. Upper and lower bounds

The results as shown in table 5.5 are based on the conducted experiment only. However, as explained in paragraph 4.3.5, by using the data that was found by Gebert in 2023, upper and lower bounds for the carbon production could be found as well. For this, the minimum and maximum produced carbon after 21 days at 20 °C, as reported by Gebert, were used and compared to this same variable, as found in the experiment that was conducted for this thesis.

As can be seen in appendix C, no measurements were carried out after exactly 21 days, but results are available for 20 days after the start of the experiment. From this, it follows that the produced carbon after 20 days, at 20 °C, was equal to 0.310 mg C/g DW, for anaerobic circumstances. As to allow for an equal comparison, the results found by Gebert were scaled by a factor 20/21, in order to reflect the carbon production after 20 days. Finally, these values were divided by the value from the experiment (0.310 mg C/g DW) as to find a maximum and minimum scaling factor. The results are shown in table 5.6.

Table 5.6: Scaling factors for upper and lower bounds of carbon generation

	21-day generation (mg C/g DW)	20-day generation (mg C/g DW)	Scaling factor (-)
Maximum	2.35	2.24	7.22
Minimum	0.25	0.24	0.77

From table 5.6, it follows that the found value of 0.310 mg C/g DW for carbon production after 20 days, at 20 °C, under anaerobic circumstances, falls within the range that was found by Gebert in 2023. The value is however towards the lower end of the spectrum.

By using the scaling factors, the values for monthly carbon generation from table 5.5 could be scaled to found the upper and lower bounds for the monthly carbon generation. The previously found values were multiplied with the scaling factors, the result is shown in table 5.7.

Table 5.7: Upper and lower bounds for monthly carbon production under anaerobic circumstances

	Temperature (°C)	Found value (mg C/g DW)	Lower bound (mg C/g DW)	Upper bound (mg C/g DW)
Jan	9.990	0.617	0.474	4.454
Feb	10.650	0.570	0.438	4.114
Mar	12.270	0.665	0.511	4.802
Apr	13.760	0.684	0.526	4.941
May	16.270	0.794	0.610	5.736
Jun	19.260	0.869	0.668	6.276
Jul	18.750	0.880	0.676	6.357
Aug	19.710	0.914	0.702	6.599
Sep	16.890	0.789	0.606	5.701
Oct	14.110	0.719	0.553	5.194
Nov	11.310	0.624	0.479	4.505
Dec	8.690	0.589	0.453	4.255

5.3. Conversion to port conditions

5.3.1. Accounting for availability of organic material

Before extrapolating the results on carbon generation to the port, the results from table 5.7 were scaled to take into account the variability of the available biomass over the year. First, this scaling factor was determined.

The results on anaerobic carbon generation in Emden, as found by Gebert in 2023, were analyzed. This gave an average carbon production of 1.01 (mg C/ g DW, after 21 days at 20 °C) for samples taken between April and October and an average production of 0.41 (mg C/ g DW, after 21 days at 20 °C) for samples taken between November and March.

This means that the generated carbon in the samples taken between November and March was found to be 0.407 that of the samples taken between April and October. Since all other parameters were the same, this shows that the amount of biomass in samples taken between November and March was 0.407 that of the samples taken in the other months.

This allows for scaling of the values found in table 5.7. As found in table 5.2, the temperature of the fluid mud layer is warmest between April and October. The samples that were used in the experiment were taken in April, which is thus a ‘warm’ month. Therefore, the found carbon production for the warmer months were not scaled. However, all ‘cold’ months (between November and March), were scaled by the found factor of 0.407, as to reflect the reduced availability of organic matter in those months, as compared to the used samples. This scaling factor was applied and the results are shown in table 5.8.

Table 5.8: Upper and lower bounds for monthly carbon production under anaerobic circumstances; scaled for availability of organic matter

	Temperature (°C)	Found value (mg C/g DW)	Lower bound (mg C/g DW)	Upper bound (mg C/g DW)
Jan	9.990	0.251	0.193	1.813
Feb	10.650	0.232	0.178	1.675
Mar	12.270	0.271	0.208	1.953
Apr	13.760	0.684	0.526	4.941
May	16.270	0.794	0.610	5.736
Jun	19.260	0.869	0.668	6.276
Jul	18.750	0.880	0.676	6.357
Aug	19.710	0.914	0.702	6.599
Sep	16.890	0.789	0.606	5.701
Oct	14.110	0.719	0.553	5.194
Nov	11.310	0.254	0.195	1.831
Dec	8.690	0.240	0.184	1.731

5.3.2. Extrapolation to the dimensions of the whole port

After the carbon production per gram of dry weight was known, this was extrapolated to the whole port. For the density of the fluid mud, data gathered by Gebert in 2023 was used. The average of all measurements was taken, which gave a density of 1.11 ton/m^3 for the dry parts of the fluid mud. For the same samples, the dry mass content was measured as well (Gebert, 2023), this gave an average dry mass content of 16.9% for the port. As was shown in figure 3.2, the fluid mud layer has a thickness of approximately 4 meters in the 'GS' part of the port and 2.5 m in the 'IH' part. Here, the average was taken, which resulted in a thickness of 3.25 m for the fluid mud layer, across the whole port. Subsequently, the area of the Port of Emden was determined by using satellite images and area measurement software. In figure 5.5, the considered area is marked in red.

Figure 5.5: Considered area Port of Emden (Google Earth, 2019)

From the area measurement software, it followed that the area of this red zone is equal to 1.72 km^2 (Google Earth, 2019). After multiplication by the found thickness of the fluid mud layer (3.25 m), it followed that the total volume of the fluid mud layer is equal to 5,590,000 m^3.

This volume was then multiplied by the known density of the fluid mud, 1.11 ton/m^3, to obtain the total mass of fluid mud (6,204,900 tons). After multiplication by the known percentage of dry matter (16.9%),

the total dry weight of the fluid mud layer was obtained (1,048,628 tons). This could finally be multiplied by the found values for carbon production per gram of dry weight, as shown in table A.5, to obtain the total produced tons of carbon for the whole port.

Table 5.9: Monthly carbon production under anaerobic circumstances in the Port of Emden

	Temperature (°C)	Found value (ton)	Lower bound (ton)	Upper bound (ton)
Jan	9.99	263	202	1901
Feb	10.65	243	187	1756
Mar	12.27	284	218	2048
Apr	13.76	717	552	5181
May	16.27	833	640	6015
Jun	19.26	911	700	6581
Jul	18.75	923	709	6666
Aug	19.71	958	736	6920
Sep	16.89	827	635	5978
Oct	14.11	754	580	5447
Nov	11.31	266	204	1920
Dec	8.69	252	193	1815

In table 5.9, the ‘Found value’ column represents the carbon production based on what was found in the experiment. The ‘Lower’ and ‘Upper bound’ columns represent lower and upper bounds for this carbon production, based on previous research by Gebert in 2023, as outlined in more detail before.

To allow for extrapolation of the results to any desired volume, the results were finally divided by the found volume of the fluid mud to obtain the carbon production per cubic meter of fluid mud. This is shown in table 5.10.

Table 5.10: Monthly carbon production under anaerobic circumstances in the Port of Emden, per volume unit of fluid mud

	Temperature (°C)	Found value (g/m^3)	Lower bound (g/m^3)	Upper bound (g/m^3)
Jan	9.99	47	36	340
Feb	10.65	43	33	314
Mar	12.27	51	39	366
Apr	13.76	128	99	927
May	16.27	149	114	1076
Jun	19.26	163	125	1177
Jul	18.75	165	127	1192
Aug	19.71	171	132	1238
Sep	16.89	148	114	1069
Oct	14.11	135	104	974
Nov	11.31	48	36	343
Dec	8.69	45	35	325

6

Discussion

In this chapter, the results are interpreted and reasons for specific found relations are given. This is done along the lines of the sub-questions and afterwards, some limitations of this thesis are discussed.

6.1. Relation between temperature and carbon generation

As was found in this thesis, the generation of carbon dioxide and methane significantly varies during the year, with production in the warmest month being around 4 times higher than during the coldest month. This difference is caused by a greater availability of organic material during the warmer months, and the temperature functions, which showed greater carbon production for higher temperatures, for the same amount of organic matter. This is due to the following process: if temperature increases, molecules gain higher average kinetic energy, which means molecules move faster and collide with greater energy. With an increased number of collisions occurring at sufficient energy levels to initiate reactions, the reaction rate rises (American Chemical Society, 2023).

In figure 5.4, the found generated carbon was plotted against the temperature at which those specific samples were kept. These plots show that a temperature decrease of 10 °C resulted in approximately half the carbon production, indicating a Q_{10} value of around 2. These findings are in line with the literature, that suggests that with every 10 °C increase in temperature, the reaction rate of biological processes approximately doubles or triples (Reyes et al., 2008). Moreover, the results are in line with those of previous studies on the Port of Hamburg. Here, the carbon generation was found to increase similarly with temperature, with the found carbon production for Emden being slightly higher.

6.2. Relation between available biomass and carbon generation

The second relevant factor that explains higher carbon production in the warmer months, is a greater availability of organic matter during summer and spring, due to primary production of biomass by photoautotrophic bateria and algae during spring and summer. This effect was captured in a scaling factor of 0.407 that was applied to the five coldest months. Effectively, this approximately halved the found carbon production for those five coldest months, compared to the warmer months. Since the difference in temperature of the fluid mud layer between the warmest and coldest month was around 10 °C, the found Q_{10} value tells that the varying production rate also effectively halved the found value for carbon production in the coldest month, when compared to the warmest month. This shows that these two causes for the varying carbon production had similar effects on the final results.

The value of 0.407 for this factor was found based on previous research by Gebert in 2023. Specifically, it was found that the measured carbon production for samples taken in the warmest months was around 2.46 times higher than for samples that were collected during the colder months. This is solely due the higher availability of degradable organic matter during the warmer months, since all samples were kept at the same temperature. This result can be supported by literature. For instance, previous research found that the Mississippi River basin contained approximately 2.7 times more dissolved organic matter during the seasons with the highest levels compared to the seasons with the lowest levels. For particulate organic matter this value was around 1.8 (Tian et al., 2015). These values are thus comparable to what was found in this thesis.

6.3. Fluid mud temperature

The first sub-question focused on the seasonal variance of the fluid mud temperature. It was found that the water in the port is warmer during summer than it is during winter, as was also the hypothesis. The difference between the temperature of the fluid mud during the warmer and cooler months is however smaller than expected. This is due to the high heat capacity of water which means it takes a lot of energy to heat up or cool down a unit of water. Furthermore, the larger the depth, the longer the delay as the temperature gradient decreases with increasing depth. This makes the water near the bottom cooler than the surface water during summer and warmer during winter, as can be seen in figure 5.2.

This result wasn't expected beforehand, but can be supported by literature, since previous research has shown that water in lakes is affected by a process called 'lake stratification'. This causes a cyclical pattern in which the water overturns every year, caused by warming/cooling of water at the top and the difference in density of water at different temperatures (Boehrer & Schultze, 2008). This can cause water at the top of a lake to be warmer than the bottom during summer and cooler during winter, as was observed from the data on the Port of Emden as well.

6.4. Limitations

Other previous research, however, showed that the organic matter content not only significantly varies between the seasons, but also varies within a season (Ye et al., 2019). In this thesis, this effect was not taken into account, as the same factor was applied to all months from October until March and all the other months were not scaled. The study by Ye from 2019 shows that this assumption most likely fails to represent reality completely, as the availability of organic matter probably differs from month to month within the summer and winter. A slight trend within the season was visible in the data gathered by Gebert et al., 2023 (appendix D, lower left of the figure), however this was too unclear to take into account, which could also be due to the fact that the system is continuously disturbed because of the recirculation dredging. This is therefore the first limitation to this thesis that must be acknowledged.

Another limitation can be found in the correction of the water temperature, as it should be noted that the found relation of fluid mud temperature versus water surface temperature was based on an incomplete dataset. For the available months, results of various measurements were available and thus a good picture could be obtained. However, some months were not available, which meant assumptions had to be made based on a correlation that was found in the available data. So, although the correlation was based on varied data gathered over the whole year and was found to be significant, it is not exactly known how the water temperature varies over depth for the months on which no data was available (January, February, March, May, June, September).

In figure 5.1, the scatter plot to find the relation was shown. In this figure, the season during which each measurement was conducted is indicated with a colour. From this, it becomes clear that the water temperature at the bottom is not only dependent on the water temperature at the surface, but also on the season. For instance, a temperature of 12 °C at depth -2 m in figure 5.1 corresponds to either approximately 11 °C at depth - 10 m during spring or approximately 15 °C during fall. This is a significant difference, but was not incorporated into the model, as it only 'translates' a temperature at the surface to a temperature at the location of the fluid mud. Although the linear fit seems to find an average for the year, as can be seen in figure 5.1, it doesn't completely take the influence of the season into account and therefore most likely underestimates the temperature and thus carbon generation during the fall and overestimates these quantities during the spring.

A third limitation to this research is in the experiment that was carried out. First of all, gas was removed from the samples on a weekly basis, due to injection for the GC measurements. This means that the carbon production found in the experiment likely underestimates reality. However, pressure of all samples was measured before and after injection, and for most samples the pressure reduction was around 1%, with 2% being the highest observed value. Therefore, the underestimation of carbon due to this effect is small. Finally, a temperature function was built based on the results of the experiment. As can be seen in figure 4.3, the temperature function for the Port of Hamburg was created based on data that was gathered over a period longer than 800 days. But for this thesis, that amount of time was not available, and data was only gathered during a period of 4 weeks. This has most likely lead to a less accurate result compared to the functions for Hamburg that were derived in previous research.

7

Conclusions and Recommendations

7.1. Conclusions

The goal of this thesis was to answer the following research question: *What is the seasonal variability of methane and carbon dioxide generation from fluid mud in the Port of Emden?* With the results that were presented in chapter 5, an answer to this question can be formulated. In order to derive a conclusion, three sub-questions were used. The conclusions relating to these sub-questions are presented first.

First, the surface water temperatures over the year in the Port of Emden were gathered from previous research and averages were taken. This data was then corrected, in order to represent the temperature at the depth of the fluid mud layer. From this, it followed that the temperature of the fluid mud layer varied between 8.69 °C in December and 19.71 °C in August, with the temperatures being highest (>13 °C) between April and October. In the other months, temperatures were found to be lower.

The second sub-question was about how the temperature variations influence methane and carbon dioxide generation in the fluid mud. For this, an experiment with samples from the Port of Emden was carried out that found the generated carbon under different temperatures. These values were compared, which showed the amount of generated carbon decreased as temperatures got lower. More specifically, a temperature decrease of 10 °C resulted in approximately half the carbon production, which corresponds to a Q_{10} value of around 2. This finding is according to the hypothesis.

In the third and final sub-question, the found carbon generation per unit of dry weight was converted into results that hold for the whole port. Here, it was found that, due to a greater availability of organic matter during the warmer months, a scaling factor had to be applied to the results on carbon generation that were found in the experiment. The need for this factor was included in the hypothesis. Finally, results were extrapolated to the whole port, based on data on density, thickness and area of the fluid mud layer. This lead to results on the total carbon production from the fluid mud layer in the Port of Emden per month.

Based on the experiment, the generated carbon in the Port of Emden, due to micro-organisms in the fluid mud layer, was found to differ between 243 tons in February and 958 tons in August. From April until October, carbon generation was found to be considerably higher (between 717 and 958 tons) than from November until March (between 243 and 284 tons). Based on data that was gathered by previous research, plausible upper and lower bounds for the carbon production were determined per month. The upper bound was found to be 7.2 times greater than the values found in the experiment and the lower bound was 1.3 times smaller than the found values.

Finally, the found results for aerobic conditions were not presented in chapter 5, but are shown in appendix A. After comparing these results to the anaerobic results from chapter 5, it follows that carbon production under aerobic conditions was found to be around 2.7 to 2.8 times higher than under anaerobic conditions, with the same variability over the year. Exact results are given in appendix A.

7.2. Recommendations

As was discussed in chapter 6, a couple of limitations to this thesis must be acknowledged. Further research could first of all focus on these limitations, for instance on gathering more data on the seasonal variations in organic matter and fluid mud temperature in the Port of Emden. With this, a more complete picture of the governing circumstances can be obtained. After all, right now there is a 'gap' in the temperature data between January and March and the month to month variability of organic matter was not taken into account. With more data on this, a more accurate representation of the seasonal variance in carbon generation can be given.

Further research could also focus on deriving a more reliable temperature function for the Port of Emden that relates time to generated carbon at different temperatures. For this, more temperatures between 10 °C and 20 °C should be included, as this thesis found that these temperatures are most relevant for the port. If more relevant temperatures are researched, a more complete picture of the temperature function of the Emden fluid mud layer can be obtained. Moreover, data on carbon generation should be gathered for a longer period of time than was done in this thesis, to increase reliability of the results. Finally, further research could explore how the results from this study can be applied. For instance, how can sediment management activities be altered in order to lower the carbon generation, especially in months during which this generation is high?

References

American Chemical Society. (2023, August). Temperature and the Rate of a Chemical Reaction. https://www.acs.org/middleschoolchemistry/lessonplans/chapter6/lesson4.html#:~:text=When%20the%20reactants%20are%20heated,rate%20of%20the%20reaction%20increases.

Arndt, S., & LaRowe, D. E. (2017, October). *Organic matter degradation and preservation*.

Bidlingmaier, W. (2016). *Biological waste treatment*.

Boehrer, B., & Schultze, M. (2008). Stratification of lakes. *Reviews of geophysics*, *46*(2). https://doi.org/10.1029/2006rg000210

Chamanmotlagh, F., Kirichek, A., & Gebert, J. (2024). *Effects of Recirculation Dredging on Density, Strength, Settling and Oxygen Concentration of Fluid Mud in the Port of Emden* (tech. rep.). Journal of Soils; Sediments, under revision.

Encyclopaedia Britannica. (2011, December). Emden. https://www.britannica.com/place/Emden-Germany

Gebert, J. (n.d.). Fluid mud picture.

Gebert, J., Deon, F., Shakeel, A., Kirichek, A., Perner, M., Böhnke-Brandt, S., Krohn, I., Bergmann, L., van Rees, F., & de Lucas Pardo, M. (2023). *Investigation of the microbiology in fluid mud of Seaport Emden (‚Emden-FM')* (tech. rep.). Report to Niedersachsen Ports.

Giard, D. (2011). Biogas production regime for in-storage psychrophilic anaerobic digestion. https://escholarship.mcgill.ca/concern/theses/tq57nv89m

Google Earth. (2019, August). Port of Emden, Emden, Germany; 53° 20' 56.66"N, 7° 12' 55.75"E, Eye alt 5.37 km. Landsat/Copernicus. http://www.earth.google.com

Haynes, W. M., Lide, D. R., & Bruno, T. J. (2014, June). *CRC Handbook of Chemistry and Physics* (95th ed.). CRC Press. https://doi.org/10.1201/b17118

Kamusoko, R., Jingura, R. M., Chikwambi, Z., & Parawira, W. (2022, January). *Biogas: microbiological research to enhance efficiency and regulation*. https://doi.org/10.1016/b978-0-12-822810-4.00025-7

Li, X. (2019, January). Investigation of Gas Generation by Riverine Sediments: Production Dynamics and Effects of Sediment Properties. http://resolver.tudelft.nl/uuid:a56b5642-f1f8-4845-b24a-eea598967698

McAnally, W., Friedrichs, C., Hamilton, D., Hayter, E., Shrestha, P., Rodriguez, H., Sheremet, A., & Teeter, A. (2007). Management of fluid mud in estuaries, bays, and lakes. i: Present state of understanding on character and behavior. *Journal of Hydraulic Engineering-asce - J HYDRAUL ENG-ASCE*, *133*. https://doi.org/10.1061/(ASCE)0733-9429(2007)133:1(9)

Menzel, T., Neubauer, P., & Junne, S. (2020). Role of Microbial Hydrolysis in Anaerobic Digestion. *Energies*, *13*(21), 5555. https://doi.org/10.3390/en13215555

Mobilian, C., & Craft, C. (2022, January). *Wetland soils: physical and chemical properties and biogeochemical processes*. https://doi.org/10.1016/b978-0-12-819166-8.00049-9

NASA. (2023, December). Methane. https://climate.nasa.gov/vital-signs/methane/?intent=121#:~:text=Methane%20(CH4)%20is%20a,carbon%20dioxide%20(CO2).

Niedersachsen Ports. (n.d.). AMISIA – Advanced Port Maintenance: Intelligent, Sustainable, innovative and Automated dredging. https://www.nports.de/media/hafenplus/Projekte/AMISIA/NPorts-Projektsteckbrief-AMISIA.pdf

Niedersachsen Ports. (2024). *The Seaport of Emden* (tech. rep.). https://www.nports.de/media/Haefen/Emden/nports-location-brochure-port-emden.pdf

Polman, E. M., Gruter, G.-J. M., Parsons, J. R., & Tietema, A. (2021). Comparison of the aerobic biodegradation of biopolymers and the corresponding bioplastics: A review. *Science of the total environment*, *753*. https://doi.org/10.1016/j.scitotenv.2020.141953

Prescott, L. M., Harley, J. P., & Klein, D. A. (1996, January). *Microbiology*.

Reyes, B. A., Pendergast, J. S., & Yamazaki, S. (2008). Mammalian peripheral circadian oscillators are temperature compensated. *Journal of biological rhythms*, *23*(1), 95–98. https://doi.org/10.1177/0748730407311855

Sikora, A., Detman, A., Chojnacka, A., & Błaszczyk, M. (2017, February). *Anaerobic Digestion: I. A Common Process Ensuring Energy Flow and the Circulation of Matter in Ecosystems. II. A Tool for the Production of Gaseous Biofuels*. https://doi.org/10.5772/64645

Singh, B., & Sharma, N. (2008). Mechanistic implications of plastic degradation. *Polymer degradation and stability*, *93*(3), 561–584. https://doi.org/10.1016/j.polymdegradstab.2007.11.008

Sudoe, E. (2022, January). What are volatile fatty acids? https://ecoval-sudoe.eu/en/what-are-volatile-fatty-acids/

Tian, H., Ren, W., Yang, J., Tao, B., Cai, W.-J., Lohrenz, S. E., Hopkinson, C. S., Liu, M., Yang, Q., Lu, C., Zhang, B., Banger, K., Pan, S., He, R., & Xue, Z. (2015). Climate extremes dominating seasonal and interannual variations in carbon export from the Mississippi River Basin. *Global biogeochemical cycles*, *29*(9), 1333–1347. https://doi.org/10.1002/2014gb005068

van Rijn, L. (2023, December). *Fluid mud formation* (tech. rep.). https://www.leovanrijn-sediment.com/papers/Fluidmudformation2016.pdf

Ye, L., Wu, X., Yan, D., Yang, B., Zhang, T., & Huang, D. (2019). Dissolved organic carbon content is lower in warm seasons and neutral sugar composition indicates its degradation in a large subtropical river (Nantong Section), China. *Environmental earth sciences*, *78*(6). https://doi.org/10.1007/s12665-019-8234-z

Zaiontz, C. (n.d.). Pearson's Correlation Table. https://real-statistics.com/statistics-tables/pearsons-correlation-table/

Zander, F. (2022). Turnover of suspended and settled organic matter in ports and waterways. https://doi.org/10.4233/uuid:f4d57842-9603-41aa950b-1009ab3c3fe3

Zander, F., Groengroeft, A., Eschenbach, A., Heimovaara, T., & Gebert, J. (2022). Organic matter pools in sediments of the tidal Elbe river. *Limnologica*, *96*, 125997. https://doi.org/10.1016/j.limno.2022.125997

A

Aerobic results

In this appendix, the results on carbon production per month for aerobic conditions are given. Here, the same procedure is applied as was outlined in 4.3, but now for aerobic conditions.

A.1. Found carbon production

The temperature function that was derived for aerobic conditions can be found in the right-hand side of figure 5.3. First, the results were compared to the findings that were obtained by Zander in 2022, for the Port of Hamburg. In this analysis, the carbon generated after 20 days was again compared across different temperatures, using data from Zander and from the experiment conducted in this thesis. The comparison is illustrated in figure A.1. On the right-hand side of figure A.1, the results are scaled relative to the carbon production observed after 20 days at 25 °C for the Emden samples. This scaling shows the decrease in carbon production with lower temperatures.

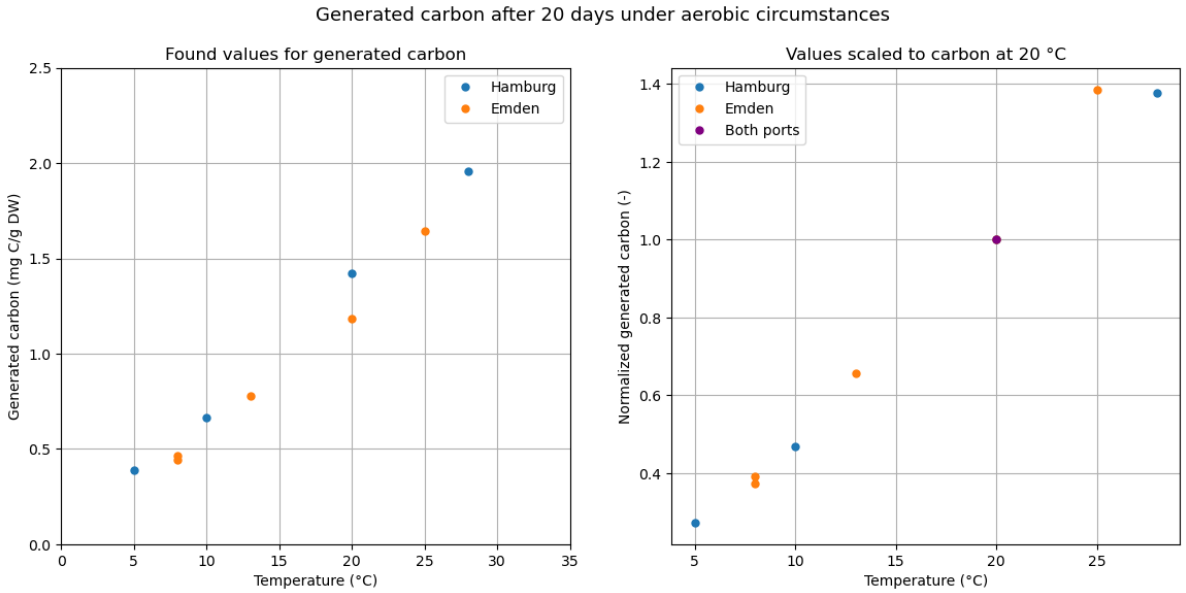

Figure A.1: Comparison of Hamburg and Emden temperature functions for aerobic circumstances

Figure A.1 shows that the samples from the Port of Emden, under aerobic circumstances, were found to produce slightly less carbon for the same temperatures than the samples from the Port of Hamburg. However, the carbon amounts found at identical temperatures were similar. The right graph demonstrates similar reactions to temperature changes. It also reveals that reducing the temperature by 10 °C, approximately halved the carbon production for the Emden samples, corresponding to a Q10 of about 2.

For aerobic conditions, the data on carbon produced after 5.96 days was used and scaled to reflect the generated carbon after exactly 5 days. The result is shown in table A.1.

Table A.1: Carbon production after 5 days under aerobic circumstances

Temperature (°C)	Generated carbon (mg C/g DW)
8	0.2461
13	0.3170
20	0.3935
25	0.5909

To estimate carbon generation in the port under aerobic conditions, monthly water temperatures from table 5.2 were compared with the nearest available results in A.1. A weighted average was calculated to determine carbon production after 5 days across all temperatures. These values were then adjusted to derive monthly carbon production, just like was done for anaerobic conditions. The result can be found in table A.2.

Table A.2: Monthly carbon production under aerobic circumstances

	Temperature (°C)	5-day generation (mg C/g DW)	Monthly generation (mg C/g DW)
Jan	9.990	0.274	1.701
Feb	10.650	0.284	1.588
Mar	12.270	0.307	1.901
Apr	13.760	0.325	1.952
May	16.270	0.353	2.187
Jun	19.260	0.385	2.312
Jul	18.750	0.380	2.355
Aug	19.710	0.390	2.420
Sep	16.890	0.359	2.157
Oct	14.110	0.329	2.041
Nov	11.310	0.293	1.758
Dec	8.690	0.256	1.586

A.2. Upper and lower bounds

Just like for anaerobic conditions, plausible upper and lower bounds were determined for aerobic conditions as well. The applied procedure, which makes use of data found by Gebert in 2023, is outlined in paragraph 4.3.5. The resulting bounds are shown in table A.3

Table A.3: Scaling factors for upper and lower bounds of carbon generation

	21-day generation (mg C/g DW)	20-day generation (mg C/g DW)	Scaling factor (-)
Maximum	4.84	4.61	3.89
Minimum	1.45	1.38	1.17

From the experiment, it followed that the produced carbon after 20 days at 20 °C, was equal to 1.185 mg C/g DW, for aerobic circumstances. Raw data can be found in appendix C . As can be seen in table A.3, the minimum bound is higher than this value from the experiment. This is why the minimum bound was adjusted to 1.185 mg C/g DW, equal to the value found in the experiment. The scaling factor for the upper bound, as shown in table A.3, was applied.

Table A.4: Upper and lower bounds for monthly carbon production under aerobic circumstances

	Temperature (°C)	Found value (mg C/g DW)	Lower bound (mg C/g DW)	Upper bound (mg C/g DW)
Jan	9.990	1.701	1.701	6.615
Feb	10.650	1.588	1.588	6.178
Mar	12.270	1.901	1.901	7.392
Apr	13.760	1.952	1.952	7.591
May	16.270	2.187	2.187	8.505
Jun	19.260	2.312	2.312	8.993
Jul	18.750	2.355	2.355	9.158
Aug	19.710	2.420	2.420	9.411
Sep	16.890	2.157	2.157	8.388
Oct	14.110	2.041	2.041	7.936
Nov	11.310	1.758	1.758	6.836
Dec	8.690	1.586	1.856	6.170

A.3. Conversion to port-conditions

In order to derive results that give information on the whole port, first the found values were accounted for the varying availability of organic matter over the year. This was done in the same matter as for the anaerobic results, so all values in 'cold' months (between November and March), were scaled by 0.407. The other values were not scaled, results are shown in table A.5.

Table A.5: Upper and lower bounds for monthly carbon production under aerobic circumstances; scaled for availability of organic matter

	Temperature (°C)	Found value (mg C/g DW)	Lower bound (mg C/g DW)	Upper bound (mg C/g DW)
Jan	9.990	0.692	0.692	2.694
Feb	10.650	0.647	0.647	2.515
Mar	12.270	0.774	0.774	3.012
Apr	13.760	1.952	1.952	7.591
May	16.270	2.187	2.187	8.505
Jun	19.260	2.312	2.312	8.993
Jul	18.750	2.355	2.355	9.158
Aug	19.710	2.420	2.420	9.411
Sep	16.890	2.157	2.157	8.388
Oct	14.110	2.041	2.041	7.936
Nov	11.310	0.716	0.716	2.784
Dec	8.690	0.645	0.755	2.513

With these values, the carbon production could be extrapolated to the whole port. This was done in the same way as for the anaerobic results and since density, thickness and area of the fluid mud layer do not differ for aerobic/anaerobic conditions, the values were again multiplied by a dry weight of 1,048,628 tons, as was found in paragraph 5.3.2. The final results on the found carbon production per month, for the Port of Emden under aerobic conditions, are shown in table A.6.

Table A.6: Monthly carbon production under aerobic circumstances in the Port of Emden

	Temperature (°C)	Found value (ton)	Lower bound (ton)	Upper bound (ton)
Jan	9.99	726	726	2825
Feb	10.65	678	678	2637
Mar	12.27	812	812	3158
Apr	13.76	2047	2047	7960
May	16.27	2293	2293	8919
Jun	19.26	2424	2424	9430
Jul	18.75	2470	2469	9603
Aug	19.71	2538	2538	9869
Sep	16.89	2262	2262	8796
Oct	14.11	2140	2140	8322
Nov	11.31	751	751	2919
Dec	8.69	676	676	2635

Finally, the results were again divided by the found volume of the fluid mud to obtain the carbon production per cubic meter of fluid mud. This is shown in table A.7.

Table A.7: Monthly carbon production under aerobic circumstances in the Port of Emden, per volume unit of fluid mud

	Temperature (°C)	Found value (g/m^3)	Lower bound (g/m^3)	Upper bound (g/m^3)
Jan	9.99	130	130	505
Feb	10.65	121	121	472
Mar	12.27	145	145	565
Apr	13.76	366	366	1424
May	16.27	410	410	1595
Jun	19.26	434	434	1687
Jul	18.75	442	442	1718
Aug	19.71	454	454	1765
Sep	16.89	405	405	1574
Oct	14.11	383	383	1489
Nov	11.31	134	134	522
Dec	8.69	121	12	471

B

Python code

B.1. Water temperatures

Here, the python code that was used for determining the water temperatures and correcting for the depth of the fluid mud layer, is shown.

```
#!/usr/bin/env python
# coding: utf-8

# In[1]:


import numpy as np
import pandas as pd
import matplotlib.pyplot as plt
import os
temps = pd.read_csv('temperatures.csv', index_col=0)
tempslist = temps.Mean.values


# In[2]:


folder_path = 'C:/Users/nieka/BEP/Temps'

dataframes = []

for filename in os.listdir(folder_path):
    if filename.endswith('.csv'):
        file_path = os.path.join(folder_path, filename)
        df = pd.read_csv(file_path, delimiter=';', usecols=[2,5])
        df.rename(columns={df.columns[0]: 'Depth', df.columns[1]: 'Temp'}, inplace=True)

        df['Depth'] = df['Depth'].str.replace(',', '.').astype(float)
        df['Temp'] = df['Temp'].str.replace(',', '.').astype(float)
        dataframes.append(df)


# In[3]:


tempsat2 = []
tempsat10 = []

for i in range(len(dataframes)):
    j = 0
    tempsatsurface = []
    df = dataframes[i]
    if abs(df.iloc[(df['Depth'] - 10).abs().argmin()]['Depth'] - 10) <= 0.05:
        index10 = df.iloc[(df['Depth'] - 10).abs().argmin()].Temp
        tempsat10.append(index10)
        index2 = df.iloc[0,1]
        tempsat2.append(index2)

```

```

# In[4]:


plt.figure(figsize=(8,5))
plt.scatter(tempsat2, tempsat10, label='Measurements')
fit = np.polyfit(tempsat2, tempsat10, 1)
fitfunc = np.poly1d(fit)
xvalues = np.linspace(min(tempsat2), max(tempsat2), 100)

residuals = tempsat10 - fitfunc(tempsat2)
SS_res = np.sum(residuals**2)
SS_tot = np.sum((tempsat10 - np.mean(tempsat10))**2)  # Corrected
r_squared = 1 - (SS_res / SS_tot)

plt.plot(xvalues, fitfunc(xvalues), color='red', label=f'Linear␣Fit;␣$R^2$:␣{r_squared:.3f}')

plt.title(f'Correlation␣between␣temperatures␣at␣depths␣-2␣m␣and␣-10␣m')
plt.xlabel('Temperature␣at␣depth␣-2␣m')
plt.ylabel('Temperature␣at␣depth␣-10␣m')
plt.grid()
plt.legend()


# In[5]:


from IPython.display import display, Math
display(Math(f'Found␣fit:␣T_{{10}}␣=␣{fit[0]:.4f}␣\cdot␣T_{{2}}␣+␣{fit[1]:.4f}'))

def tempfunc(T2):
    T10 = fit[0] * T2 + fit[1]
    return T10


# In[6]:


corrtemps = []
difftemps = []
for T2 in tempslist:
    corrtemps.append(round(tempfunc(T2),3))
    difftemps.append(round(tempfunc(T2) - T2,3))

print(corrtemps)
print(difftemps)
```

B.2. Monthly carbon production

Below, the python code used for determining the carbon production per month, as well as the upper and lower bounds, is shown.

```
#!/usr/bin/env python
# coding: utf-8

# In[1]:


import matplotlib.pyplot as plt
import pandas as pd
import numpy as np
from scipy.optimize import curve_fit
from Temperaturesfluidmud import corrtemps


# In[2]:


ae_dataham = pd.read_excel('240507_Anaerobic-aerobic␣data.xlsx', sheet_name='Aerobic-DW',
    skiprows=1)
```

```
an_dataham = pd.read_excel('240507_Anaerobic-aerobic data.xlsx', sheet_name='Anaerobic-DW',
    skiprows=1)
emdres = pd.read_excel('Berekeningen.xlsx', sheet_name='Graphs', skiprows=7)


# In[3]:


tempsham = [5, 10, 20, 28]
tempsemd = emdres.iloc[:5,0]

gencaeham = ae_dataham.iloc[3,range(1,9,2)]
gencaeemd = emdres.iloc[6:11,1]

gencaehamscaled = gencaeham / emdres.iloc[10,1]
gencaeemdscaled = gencaeemd / emdres.iloc[10,1]

fig, axes = plt.subplots(nrows=1, ncols=2, figsize=(14, 6))

axes[0].plot(tempsham, gencaeham, '.', markersize=10, label='Hamburg')
axes[0].plot(tempsemd, gencaeemd, '.', markersize=10, label='Emden')
axes[0].set_xlim(0, 35); axes[0].set_ylim(0, 2.5)
axes[0].set_xlabel('Temperature (°C)'); axes[0].set_ylabel('Generated carbon (mg C/g DW)')
axes[0].set_title('Found values for generated carbon')
axes[0].grid()
axes[0].legend()

axes[1].plot(tempsham, gencaehamscaled, '.', markersize=10, label='Hamburg')
axes[1].plot(tempsemd, gencaeemdscaled, '.', markersize=10, label='Emden')
axes[1].set_xlim(0, 35); axes[1].set_ylim(0, 1.3)
axes[1].set_xlabel('Temperature (°C)'); axes[1].set_ylabel('Normalized generated carbon (-)')
axes[1].set_title('Values scaled to carbon at 25 °C in Emden')
axes[1].grid()
axes[1].legend()
plt.suptitle('Generated carbon after 20 days under aerobic circumstances', size=13)


# In[4]:


gencanham = an_dataham.iloc[13:17, 1]
gencanemd = emdres.iloc[:5,1]

gencanhamscaled = gencanham / emdres.iloc[4,-1]
gencanemdscaled = gencanemd / emdres.iloc[4,-1]

fig, axes = plt.subplots(nrows=1, ncols=2, figsize=(14, 6))

axes[0].plot(tempsham, gencanham, '.', markersize=10, label='Hamburg')
axes[0].plot(tempsemd, gencanemd, '.', markersize=10, label='Emden')
axes[0].set_xlim(0, 35); axes[0].set_ylim(0, 0.65)
axes[0].set_xlabel('Temperature (°C)'); axes[0].set_ylabel('Generated carbon (mg C/g DW)')
axes[0].set_title('Found values for generated carbon')
axes[0].grid()
axes[0].legend()

axes[1].plot(tempsham, gencanhamscaled, '.', markersize=10, label='Hamburg')
axes[1].plot(tempsemd, gencanemdscaled, '.', markersize=10, label='Emden')
axes[1].set_xlim(0, 35); axes[1].set_ylim(0, 1.1)
axes[1].set_xlabel('Temperature (°C)'); axes[1].set_ylabel('Normalized generated carbon (-)')
axes[1].set_title('Values scaled to carbon at 25 °C in Emden')
axes[1].grid()
axes[1].legend()
plt.suptitle('Generated carbon after 20 days under anaerobic circumstances', size=13)


# In[5]:


genc5daysanemd = emdres.iloc[13:17,1]
genc5daysaeemd = emdres.iloc[19:,1]
```

```
88
89
90  # In[6]:
91
92
93  fivedayprodan = []
94  fivedayprodae = []
95  for temp in corrtemps:
96      if 8 < temp < 13:
97          prodan = abs(temp - 13) / (13 - 8) * genc5daysanemd.iloc[0] + abs(temp - 8) / (13 -
                8) * genc5daysanemd.iloc[1]
98          prodae = abs(temp - 13) / (13 - 8) * genc5daysaeemd.iloc[0] + abs(temp - 8) / (13 -
                8) * genc5daysaeemd.iloc[1]
99
100     elif 13 < temp < 20:
101         prodan = abs(temp - 20) / (20 - 13) * genc5daysanemd.iloc[1] + abs(temp - 13) / (20 -
                13) * genc5daysanemd.iloc[2]
102         prodae = abs(temp - 20) / (20 - 13) * genc5daysaeemd.iloc[1] + abs(temp - 13) / (20 -
                13) * genc5daysaeemd.iloc[2]
103     fivedayprodan.append(prodan)
104     fivedayprodae.append(prodae)
105
106
107 # In[7]:
108
109
110 months = ['jan', 'feb', 'mar', 'apr', 'may', 'jun', 'jul', 'aug', 'sep', 'oct', 'nov', 'dec']
111 daysinmonth = [31, 28, 31, 30, 31, 30, 31, 31, 30, 31, 30, 31]
112 i = 0
113 prodlistae = []; prodlistan = []
114
115 for days in daysinmonth:
116     monthlyprodae = days / 5 * fivedayprodae[i]
117     monthlyprodan = days / 5 * fivedayprodan[i]
118     prodlistae.append(monthlyprodae)
119     prodlistan.append(monthlyprodan)
120     i += 1
121
122
123 # In[8]:
124
125
126 print('Under␣anaerobic␣circumstances:')
127 j = 0
128 for month in months:
129     print(f'In␣{month},␣anaerobic␣carbon␣production␣is:␣{prodlistan[j]:.3f}␣mg␣C/g␣DW')
130     j += 1
131
132
133 # In[9]:
134
135
136 print('Under␣aerobic␣circumstances:')
137 j = 0
138 for month in months:
139     print(f'In␣{month},␣aerobic␣carbon␣production␣is:␣{prodlistae[j]:.3f}␣mg␣C/g␣DW')
140     j += 1
141
142
143 # In[10]:
144
145
146 reportmaxae = 4.84
147 reportminae = 1.45
148 reportmaxan = 2.35
149 reportminan = 0.25
150
151
152 # In[11]:
153
154
```

```
155 reportmaxae20 = reportmaxae * 20/21
156 reportminae20 = reportminae * 20/21
157 reportmaxan20 = reportmaxan * 20/21
158 reportminan20 = reportminan * 20/21
159
160
161 # In[12]:
162
163
164 foundae20 = gencaeemd.iloc[3]
165 foundan20 = gencanemd.iloc[3]
166 maxscaleae = reportmaxae20 / foundae20
167 minscaleae = reportminae20 / foundae20
168 maxscalean = reportmaxan20 / foundan20
169 minscalean = reportminan20 / foundan20
170
171
172 # In[13]:
173
174
175 i = 0
176 minlistae = []; minlistan = []; maxlistae = []; maxlistan = []
177
178 for days in daysinmonth:
179     maxmonthlyprodae = days / 5 * fivedayprodae[i] * maxscaleae
180     minmonthlyprodae = days / 5 * fivedayprodae[i] * minscaleae
181     maxmonthlyprodan = days / 5 * fivedayprodan[i] * maxscalean
182     minmonthlyprodan = days / 5 * fivedayprodan[i] * minscalean
183     maxlistae.append(maxmonthlyprodae); minlistae.append(minmonthlyprodae); maxlistan.append(
            maxmonthlyprodan); minlistan.append(minmonthlyprodan)
184     i += 1
```

C

Raw data

In this appendix, the raw data that was gathered in the experiments is shown. In table C.1, the mass of fluid mud that was used for each sample is shown, along with the naming and coding system that was used. In table C.2, the measured data for determining the water content of the samples is shown.

Table C.1: Used mass per sample

Label	Name	Mass sample (g)
1	4-AE-a	14.31
2	4-AE-b	15.82
3	4-AN-a	108.42
4	4-AN-b	102.55
5	8-AE-a	14.8
6	8-AE-a	16.91
7	8-AN-a	103.15
8	8-AN-b	101.39
9	13-AE-a	15.24
10	13-AE-b	15.15
11	13-AN-a	100.27
12	13-AN-b	97.32
13	20-AE-a	14.57
14	20-AE-b	15.79
15	20-AN-a	103.3
16	20-AN-b	107.53
17	25-AE-a	16.32
18	25-AE-b	15.85
19	25-AN-a	98.46
20	25-AN-b	97.2

Table C.2: Water content data

	Mass (g)
Mass tray	2.15
Total mass	71.99
Mass before	69.84
Dry mass	12.93
Wet mass	56.91
Gravimetric water content	440.14 (-)

Table C.3 shows the data that was gathered weekly from the GC and the pressure gauge. Pressures are given in hPa and the content of the gases is given in volumetric percentage.

Table C.3: Data from GC and pressure gauge

Sample	Date	Time	Patm	Pbefore	Pafter	CH4	CO2	N2	O2
1	8-5-2024	14:00	1025.3	1090.6	1101.5	0	0.43	77.24	19.94
1	14-5-2024	17:00	999.9	1069.5	1075.6	0	0.533	76.949	19.637
1	22-5-2024	14:00	1004.3	1039.9	1031.6	0	0.692	78.799	19.691
1	29-5-2024	11:30	1005.4	1038.7	1027.2	0	0.82	78.068	19.322
1	5-6-2024	14:30	1010.5	1011.2	1001.9	0	0.98	77.99	18.93
2	8-5-2024	14:00	1025.3	1073.3	1086.3	0	0.429	77.546	19.95
2	14-5-2024	17:00	999.9	1057.3	1073.9	0	0.55	77.067	19.617
2	22-5-2024	14:00	1004.3	1043	1021.2	0	0.726	78.633	19.568
2	29-5-2024	11:30	1005.4	1024	1014.5	0	0.904	78.084	19.131
2	5-6-2024	14:30	1010.5	997.6	985.5	0	1.04	77.89	18.83
3	8-5-2024	14:00	1025.3	981.4	985.4	0	0.494	98.824	1.027
3	14-5-2024	17:00	999.9	1068.6	1081.8	0	0.62	98.5	0.491
3	22-5-2024	14:00	1004.3	1055.3	1049.2	0	0.751	100.245	0.632
3	29-5-2024	11:30	1005.4	1050.4	1043.6	0	0.829	99.959	0.366
3	5-6-2024	14:30	1010.5	1038.1	1031.7	0	0.88	99.27	0.54
4	8-5-2024	14:00	1025.3	984.2	994.6	0	0.468	99.412	0.558
4	14-5-2024	17:00	999.9	1064.7	1079.9	0	0.548	99.546	0
4	22-5-2024	14:00	1004.3	1060.7	1054.5	0	0.544	100.923	0
4	29-5-2024	11:30	1005.4	1054.9	1048	0	0.551	100.669	0
4	5-6-2024	14:30	1010.5	1043.4	1036.9	0	0.56	100.28	0.07
5	8-5-2024	14:00	1025.3	1068.6	1060.2	0	0.402	77.212	19.815
5	14-5-2024	17:00	999.9	1061.1	1056.7	0	0.524	76.847	19.444
5	22-5-2024	14:00	1004.3	1043.6	1033.3	0	0.662	77.882	19.394
5	29-5-2024	11:30	1005.4	1021.7	1014.6	0	0.813	78.284	19.148
5	5-6-2024	14:30	1010.5	1010.3	1000.5	0	0.99	78.32	18.73
6	8-5-2024	14:00	1025.3	1074.5	1068.8	0	0.445	77.192	19.73
6	14-5-2024	17:00	999.9	1069.8	1060.4	0	0.55	77.176	19.461
6	22-5-2024	14:00	1004.3	1047.5	1036.1	0	0.716	77.997	19.214
6	29-5-2024	11:30	1005.4	1032.5	1021.3	0	0.909	78.409	18.988
6	5-6-2024	14:30	1010.5	1013.6	1002.6	0	1.11	78.36	18.54
7	8-5-2024	14:00	1025.3	979.7	974.5	0	0.399	98.515	1.203
7	14-5-2024	17:00	999.9	1062.1	1057.6	0	0.464	98.575	0.928
7	22-5-2024	14:00	1004.3	1049.3	1043.7	0	0.515	99.636	0.617
7	29-5-2024	11:30	1005.4	1041.8	1035.7	0	0.553	99.83	0.689
7	5-6-2024	14:30	1010.5	1034.3	1028.7	0	0.61	99.23	0.59
8	8-5-2024	14:00	1025.3	985.2	979.9	0	0.469	98.322	1.243
8	14-5-2024	17:00	999.9	1092.5	1087.4	0	0.495	98.537	0.931
8	22-5-2024	14:00	1004.3	1076.4	1069.6	0	0.568	99.417	0.739
8	29-5-2024	11:30	1005.4	1071.4	1063.4	0	0.601	99.638	0.787
8	5-6-2024	14:30	1010.5	1059.9	1053.1	0	0.62	99.2	0.75
9	8-5-2024	14:00	1025.3	1095.1	1082.3	0	0.552	77.241	19.575
9	15-5-2024	08:30	999.9	1077.8	1066.5	0	0.826	78.534	19.402
9	22-5-2024	14:00	1004.3	1058.2	1046.6	0	1.22	78.34	18.629
9	29-5-2024	11:30	1005.4	1042.3	1033.8	0	1.407	78.798	18.127
9	5-6-2024	14:30	1010.5	1029.3	1016.8	0	1.41	78.48	18.07
10	8-5-2024	14:00	1025.3	1049.2	1042.7	0	0.543	77.278	19.687
10	15-5-2024	08:30	999.9	1036.5	1026.7	0	0.816	78.171	19.399
10	22-5-2024	14:00	1004.3	1016.3	1005.7	0	1.163	78.215	18.706
10	29-5-2024	11:30	1005.4	1004.6	989.8	0	1.192	78.544	18.75
10	5-6-2024	14:30	1010.5	987.2	973.7	0	1	78.16	18.83

Sample	Date	Time	Patm	Pbefore	Pafter	CH4	CO2	N2	O2
11	8-5-2024	14:00	1025.3	993.5	987.3	0	0.494	98.515	1.281
11	15-5-2024	08:30	999.9	1086.4	1080.1	0	0.649	99.48	0.998
11	22-5-2024	14:00	1004.3	1076.1	1068.4	0	0.728	99.291	0.762
11	29-5-2024	11:30	1005.4	1062.8	1054.5	0	0.77	99.235	0.947
11	5-6-2024	14:30	1010.5	1056.1	1048.8	0	0.82	98.98	0.69
12	8-5-2024	14:00	1025.3	992.7	985.8	0	0.544	97.373	2.072
12	15-5-2024	08:30	999.9	1088.6	1081.8	0	0.7	98.895	1.207
12	22-5-2024	14:00	1004.3	1075.9	1069	0	0.783	98.755	1.178
12	29-5-2024	11:30	1005.4	1062.4	1055.7	0	0.843	98.878	1.162
12	5-6-2024	14:30	1010.5	1056.4	1048.1	0	0.91	98.57	1.04
13	8-5-2024	14:00	1025.3	1114.2	1006.2	0	0.648	78.557	19.868
13	14-5-2024	17:00	999.9	1098.1	1088	0	1.171	77.239	18.615
13	22-5-2024	14:00	1004.3	1078	1064.2	0	1.755	80.885	18.56
13	29-5-2024	11:30	1005.4	1058.7	1046.3	0	2.033	78.805	17.574
13	5-6-2024	14:30	1010.5	1039.1	1023.8	0	2.31	78.72	17.05
14	8-5-2024	14:00	1025.3	1080.7	1071.5	0	0.7	78.223	19.776
14	14-5-2024	17:00	999.9	1097.2	1087.1	0	1.199	77.311	18.635
14	22-5-2024	14:00	1004.3	1075.7	1061.4	0	1.852	81.737	18.577
14	29-5-2024	11:30	1005.4	1058.9	1045.8	0	2.141	78.851	17.333
14	5-6-2024	14:30	1010.5	1036	1022.4	0	2.46	78.72	16.77
15	8-5-2024	14:00	1025.3	1008.5	1002.1	0	0.699	99.093	1.042
15	14-5-2024	17:00	999.9	1095.2	1087.9	0	0.892	98.42	0.4
15	22-5-2024	14:00	1004.3	1085.7	1077.5	0	1.128	101.169	0.758
15	29-5-2024	11:30	1005.4	1073.1	1065.8	0	1.264	99.06	0.553
15	5-6-2024	14:30	1010.5	1066.6	1057.9	0	1.43	98.68	0.48
16	8-5-2024	14:00	1025.3	1004.3	999.4	0	0.754	98.85	1.22
16	14-5-2024	17:00	999.9	1101.6	1096.9	0	0.944	97.54	1.09
16	22-5-2024	14:00	1004.3	1093.6	1086.1	0	1.259	100.359	0.906
16	29-5-2024	11:30	1005.4	1084.9	1092.7	0	1.392	98.891	0.715
16	5-6-2024	14:30	1010.5	1073.4	1065	0	1.54	98.59	0.54
17	8-5-2024	14:00	1025.3	1153.3	1140.2	0	1.013	77.171	18.975
17	15-5-2024	08:30	999.9	1131.8	1108	0	2.001	84.521	19.36
17	22-5-2024	14:00	1004.3	1103.5	1085.8	0	2.535	78.775	16.772
17	29-5-2024	11:30	1005.4	1081.2	1068.9	0	3.049	79.294	16.067
17	5-6-2024	14:30	1010.5	1062	1041.6	0	3.58	79.51	15.12
18	8-5-2024	14:00	1025.3	1146.3	1132.1	0	0.992	77.164	19.002
18	15-5-2024	08:30	999.9	1124.9	1103	0	1.912	83.026	19.104
18	22-5-2024	14:00	1004.3	1096.1	1080.4	0	2.43	78.579	16.906
18	29-5-2024	11:30	1005.4	1076.5	1062.3	0	2.888	79.229	16.383
18	5-6-2024	14:30	1010.5	1060.2	1043.4	0	3.31	79.12	15.67
19	8-5-2024	14:00	1025.3	1025.8	1037.2	0	1.074	97.544	1.186
19	15-5-2024	08:30	999.9	1028.8	1019.4	0	1.627	102.187	1.46
19	22-5-2024	14:00	1004.3	1020.8	1012.1	0	2.016	97.307	0.996
19	29-5-2024	11:30	1005.4	1012.3	1005.2	0	2.34	99.806	0.857
19	5-6-2024	14:30	1010.5	1005.3	995.6	0	2.58	97.24	0.54
20	8-5-2024	14:00	1025.3	1025.5	1036.9	0	1.079	98.055	0.801
20	15-5-2024	08:30	999.9	1028.5	1019.5	0	1.622	101.397	1.031
20	22-5-2024	14:00	1004.3	1019	1011.1	0	2.015	98.243	0.349
20	29-5-2024	11:30	1005.4	1011.8	1003.8	0	2.239	97.602	0.729
20	5-6-2024	14:30	1010.5	1004.2	994.8	0	2.43	97.87	0.2

D

Used results from previous research

The following graph was obtained from previous research (Gebert et al., 2023) and was used to determine the upper and lower bounds of the carbon production, as well as the scaling factor that takes into account the varying availability of organic matter.

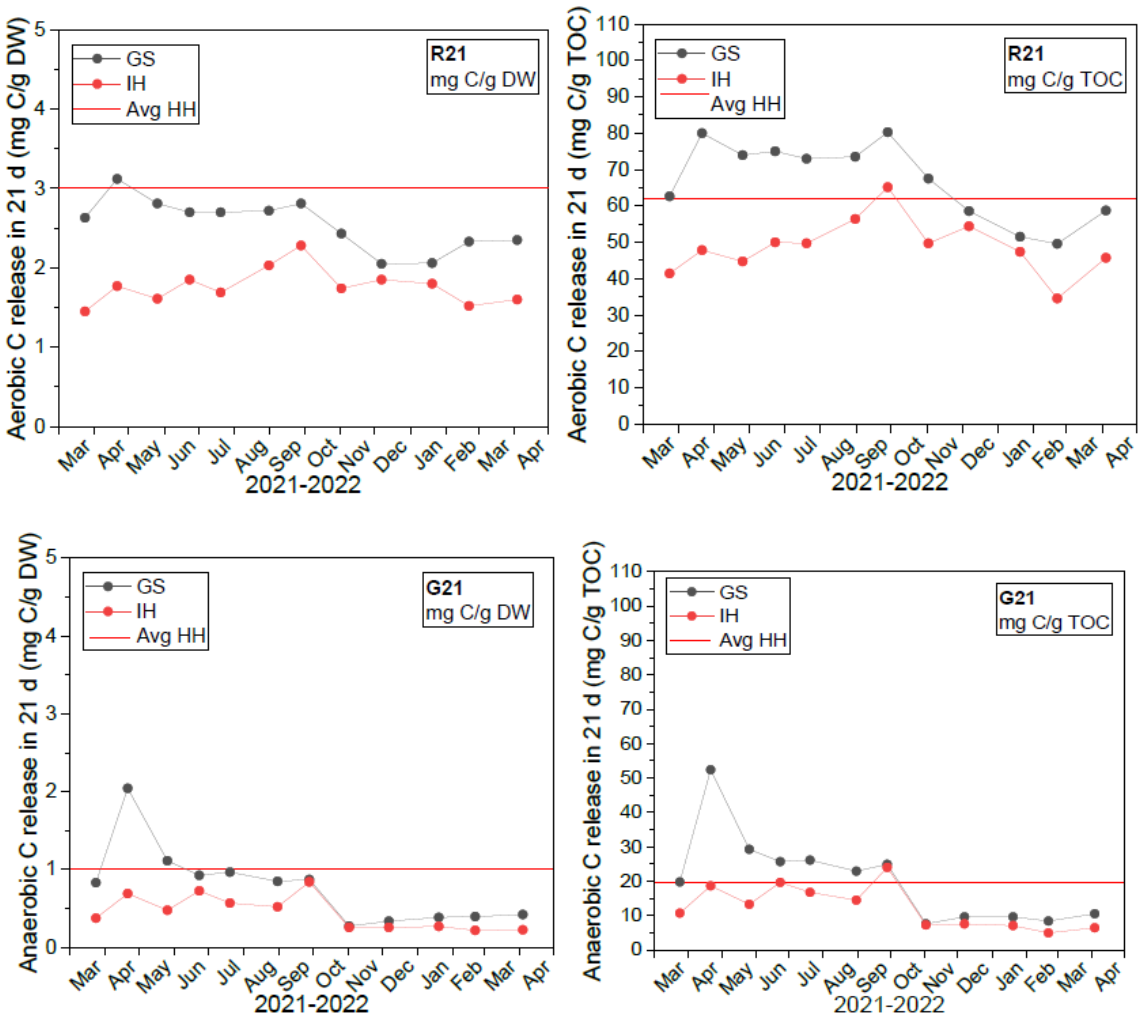

Figure D.1: Cumulative release of organic carbon in 21 days under aerobic (top) and anaerobic (bottom) conditions. Left: C release normalized to unit dry weight, Right: C release normalized to unit total organic carbon (degradability). All data valid for 20 °C. Red line: Average value for fluid mud in the Port of Hamburg (Gebert et al., 2023)